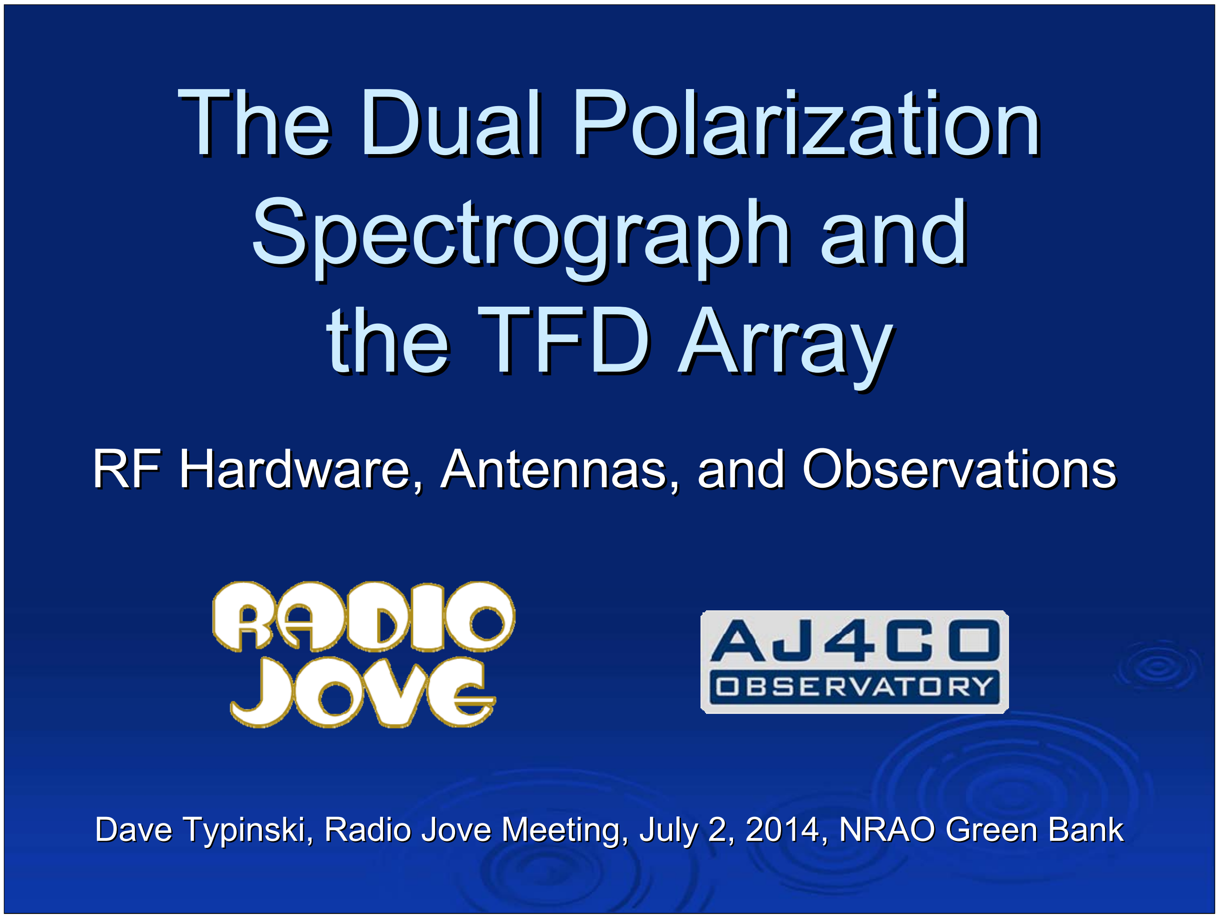

A discussion of spectropolarimetry (measuring polarization using correlated spectrographs) began in August, 2011 between Flagg and Typinski, in a coffee shop in downtown Honolulu. Jim Sky quickly became part of the project. About two years and many man-hours later, the three of us made the DPS a reality. The RF hardware was designed and built by Richard Flagg; the software and firmware were written by Jim Sky; the antenna array was designed and built by Typinski.

The DPS is really a system of components: the antenna, the receiver, and the software.

While the DPS system has produced great results during its first Jupiter season (2013-14), characterization and testing continues along with ongoing development of software tools for data analysis.

Why?

- A desire to make polarization measurements over a relatively wide bandwidth (17–33 MHz).
  - To see what there is to see!
    - Remove / reduce Faraday banding
    - Do modulation lanes appear the same?
    - What about N events?
    - Solar?
  - Why should Nancay have all the ground-based spectropolarimetry fun?

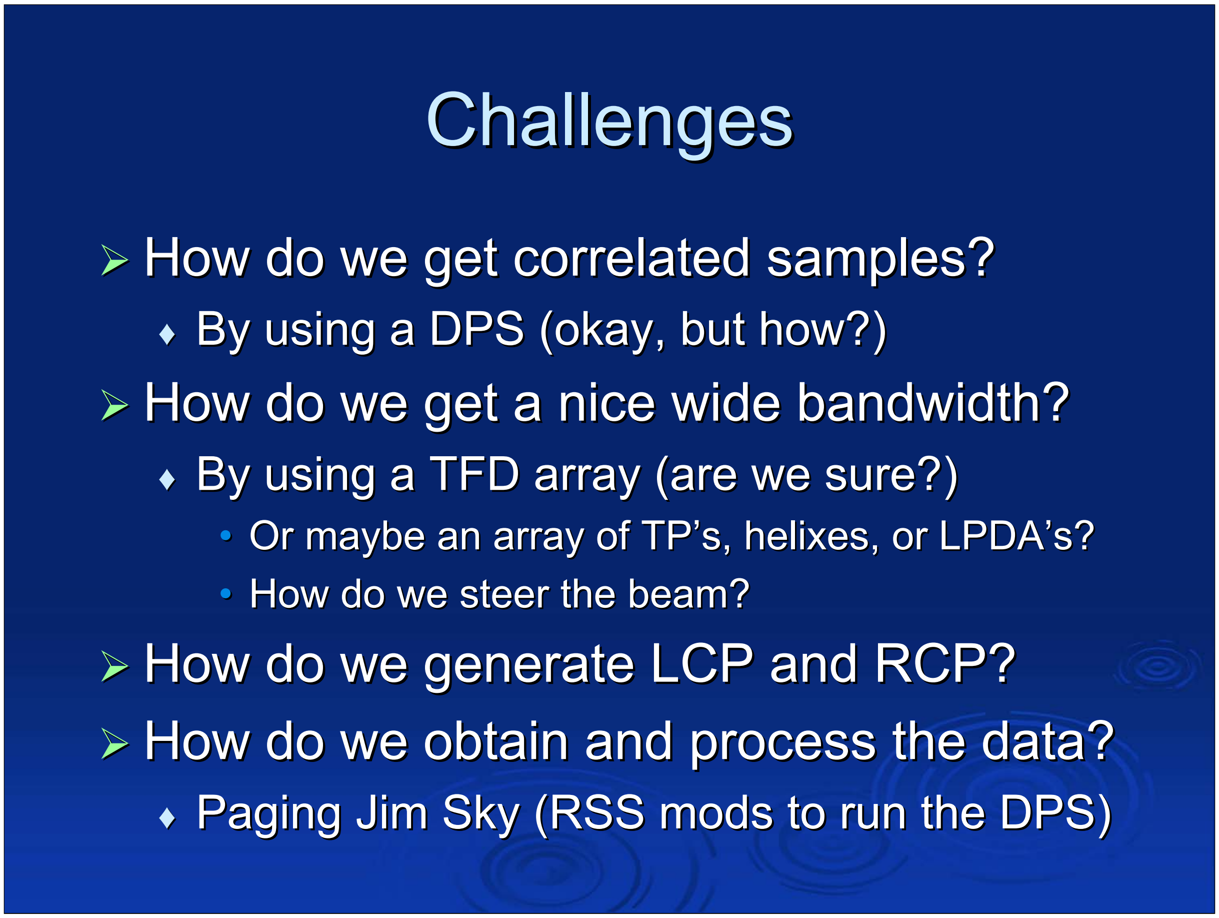

The following slides outline our answers (to date) to these challenges.

RF Hardware & Software

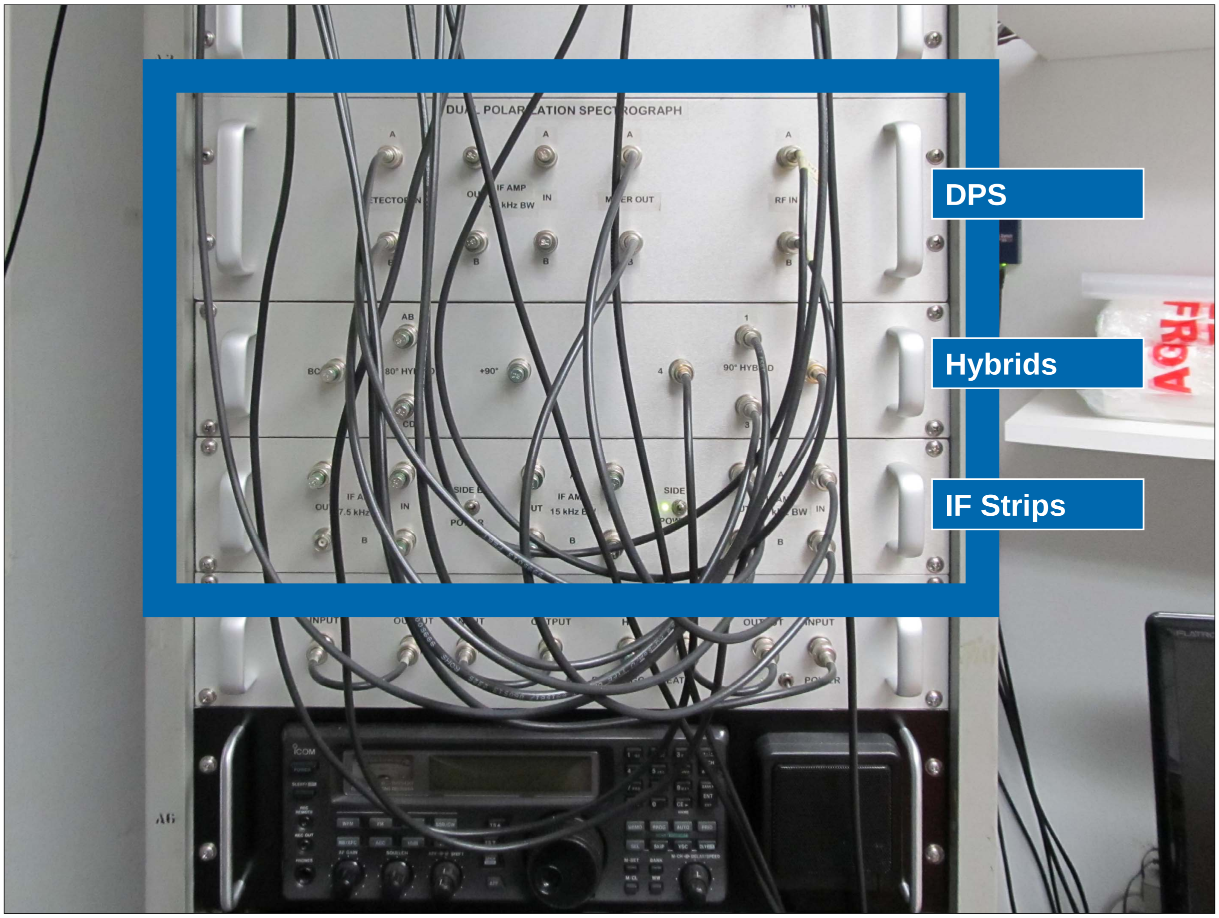

There’s a DPS is in there somewhere....

The top panel is the main DPS unit.

The middle panel contains a 10.7 MHz 180° hybrid (left) and a wideband 90° hybrid (right).

The bottom panel contains three pairs of auxiliary IF strips, two strips each of 7.5, 15, and 60 kHz bandwidth. The IF strips in the main DPS unit have a 30 kHz BW.

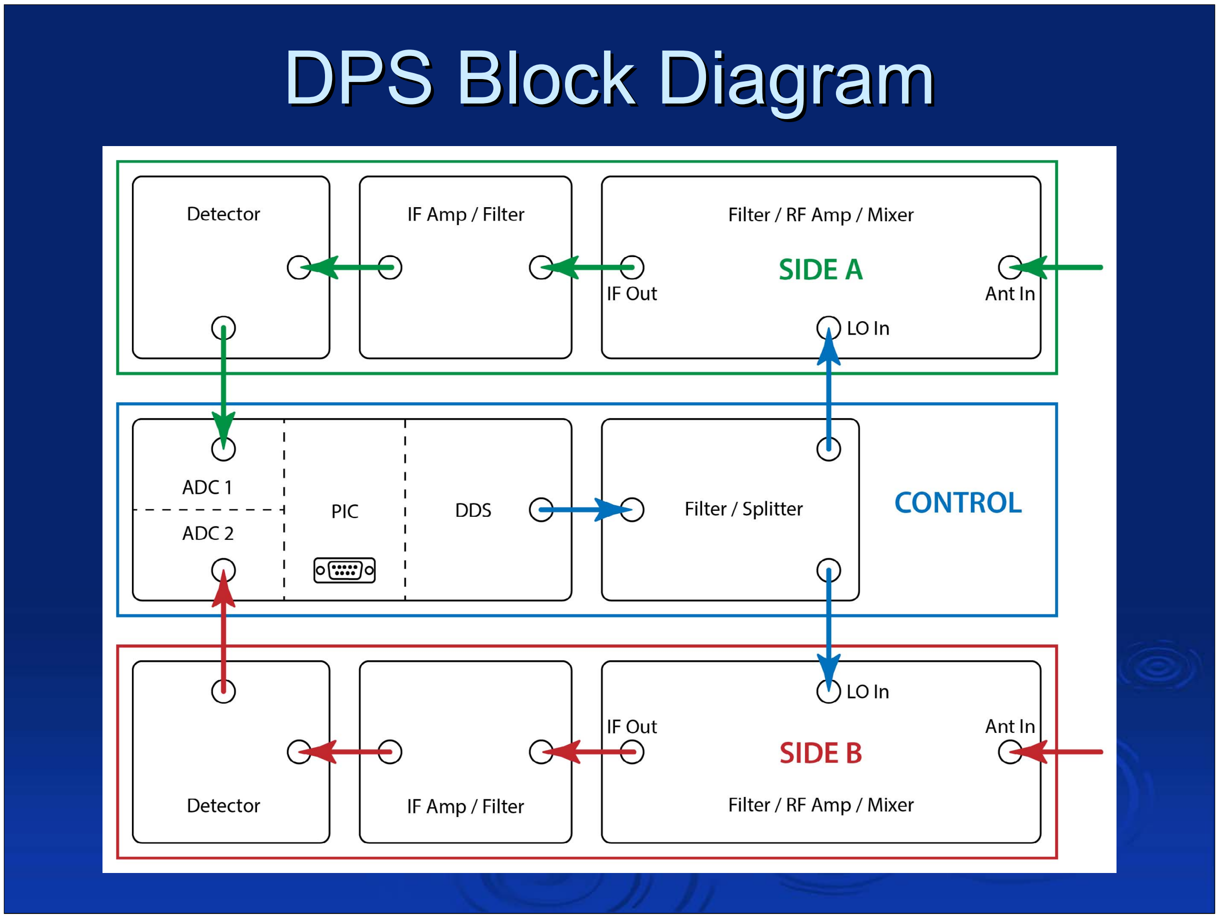

The design is basically two FSX spectrographs (as discussed in the Advanced Systems talk) tied together with a common DDS LO and controlled by a single PIC. The ADC's of each side are triggered simultaneously. The samples from the ADC in each "side" of the DPS are thus correlated, making it possible to obtain meaningful results from mathematical operations on the samples from each side (cross polarization ratio and total power).

The DPS includes 30 kHz IF amps/filters on the FSX panels. A set of auxiliary IF strips with 7.5, 15, and 60 kHz bandwidths is also used.

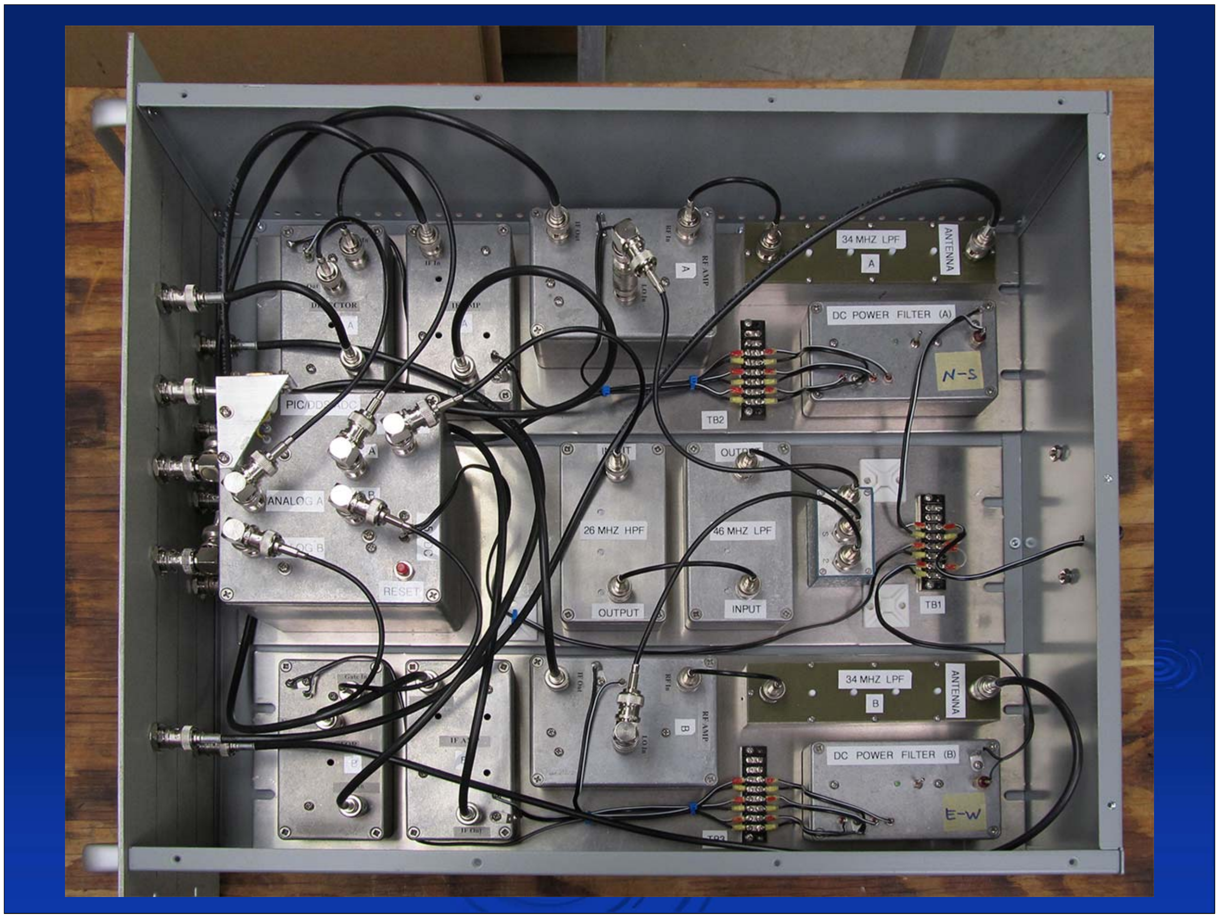

The three DPS blocks shown in the previous diagram installed in a 19” chassis.

Rear: DPS 10.7 MHz 180° hybrid ring made from 112 feet of RG-6 75 ohm coax. The letters on the masking tape labels correspond to the lettering of the wire segments shown on slides that follow. The small inner ring is a 90° RG-58 50 ohm coax phase delay cable that precedes one of the larger ring's inputs (as shown on the same slides). Connection of the narrowband 10.7 MHz hybrid is discussed on slides that follow.

Front: The small gold-colored device is a wideband hybrid, Synergy Microwave P/N DQK-701B. Connection of the wideband hybrid is discussed on slides that follow.

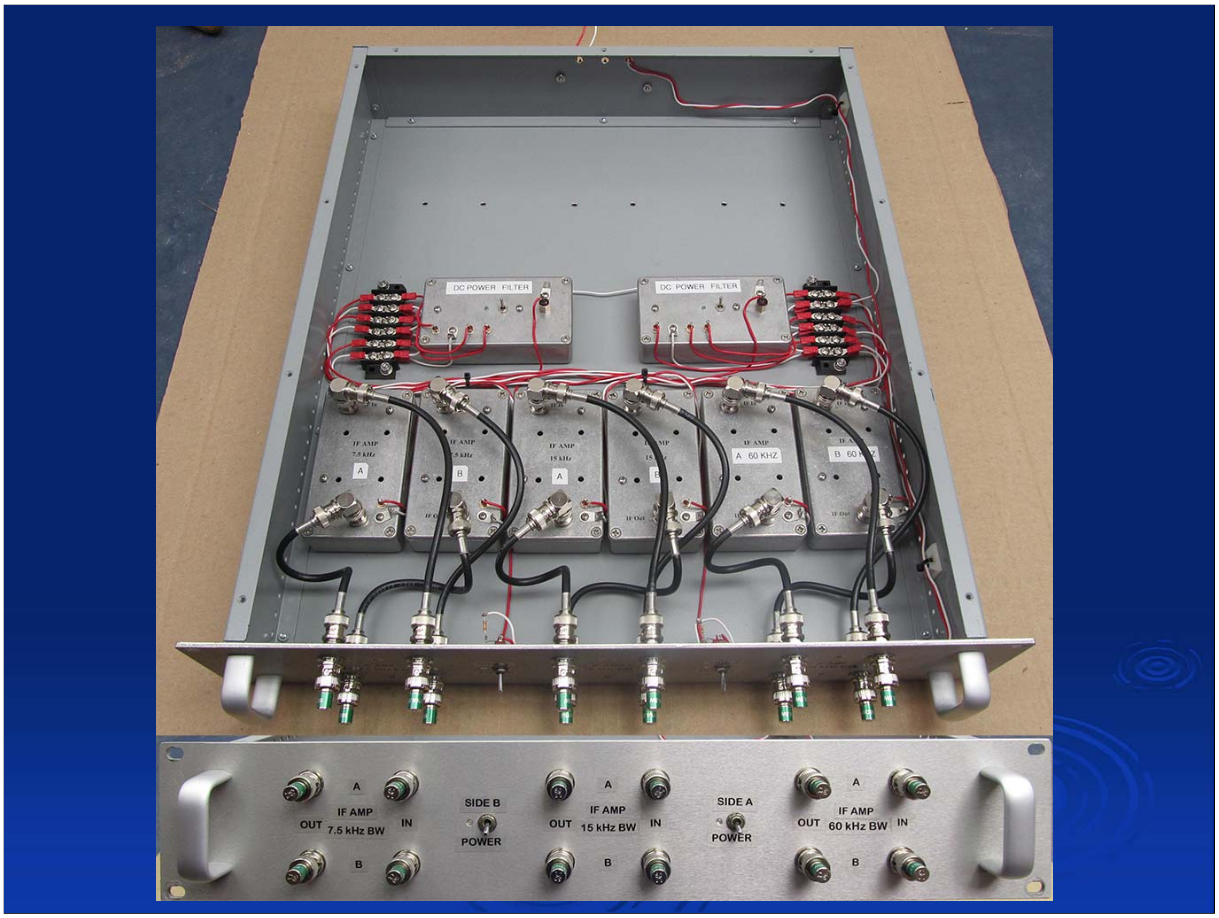

Here is a picture of the DPS auxiliary IF strip chassis. There are three pairs of aux IF strips, one for each side of the DPS at 7.5, 15, and 60 kHz bandwidth. The two 30 kHz wide IF strips are in the main DPS unit.

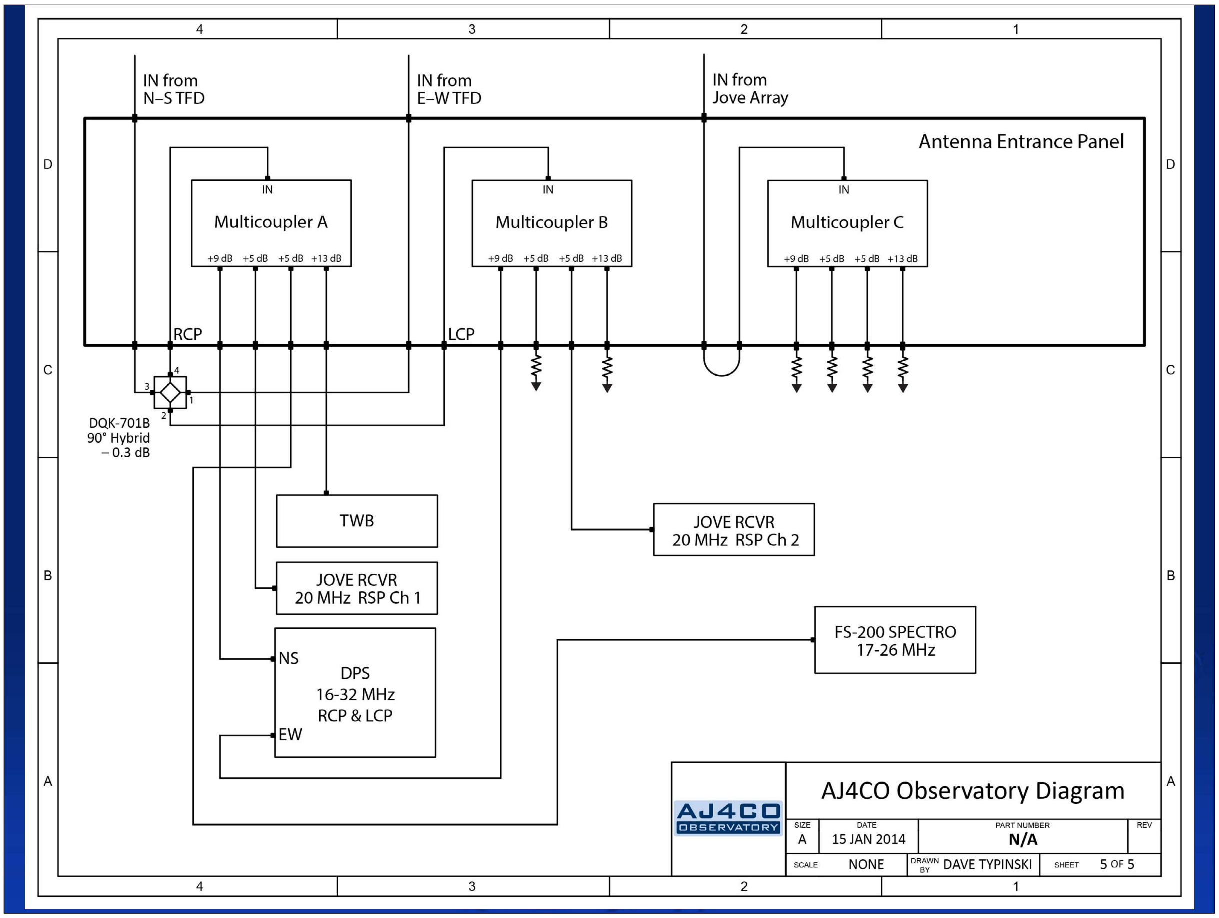

Shown here is the observatory antenna connection and signal distribution schematic.

Refer to the TWB presentation for a description of the multicouplers.

RCP and LCP are extracted from the TFD array by means of a Synergy Microwave DQK-701B wideband 90° hybrid before being passed to multicouplers A (RCP) and B (LCP), which in turn feed the two sides of the DPS.

The DPS is connected to the +9 dB output ports of MC A for RCP and MC B for LCP

RSS Software

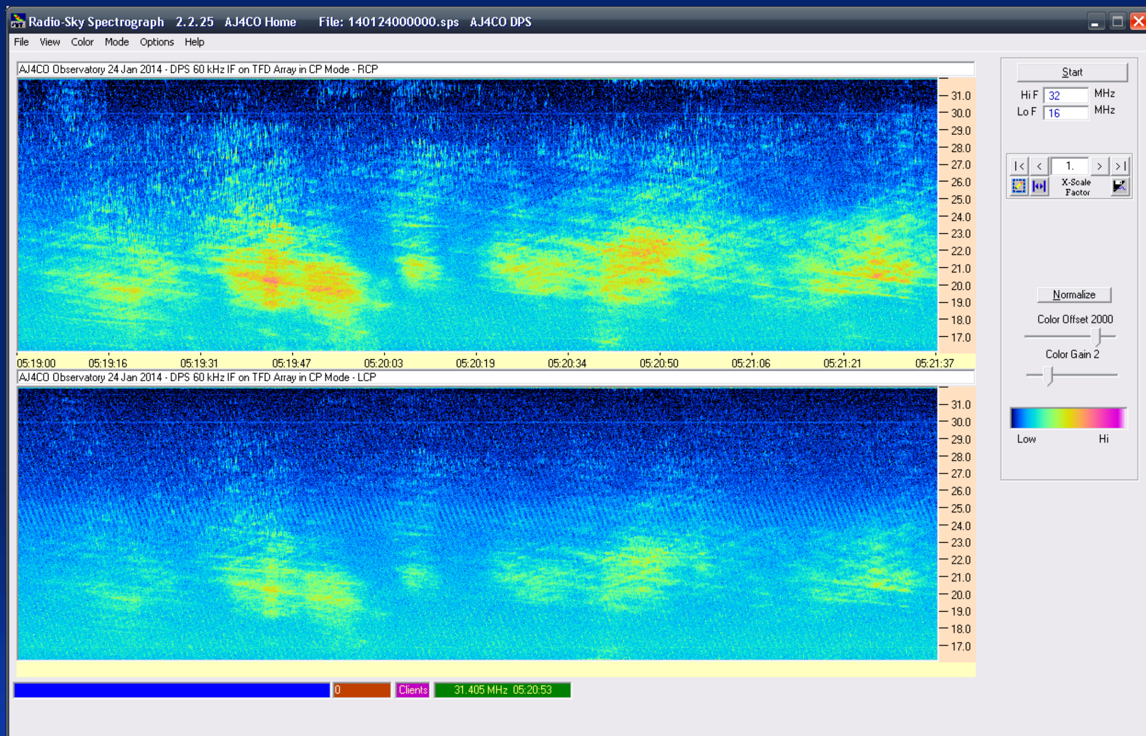

The DPS hardware is controlled by the Radio Sky Spectrograph (RSS) software. Jim Sky, who graciously makes RSS available to all for free, made several modification to RSS to allow it to control the DPS, record two correlated spectral data streams, and display two waterfalls in real time.

Here is a screen shot of RSS while running the DPS hardware. In this image, RCP is on top and LCP is on the bottom. The spectrograms in this image cover 16-32 MHz in 300 channels and a time span of 1,000 sweeps – about 2½ minutes. This was an Io-B storm of Jan 24, 2014.

This shows one of the nicer features of using circular polarization to observe Jupiter – no Faraday banding from Earth’s ionosphere (discussed in the Advanced Systems talk).

Generating RCP and LCP

Let’s talk a little bit about how RCP and LCP are obtained from a combination of linear antennas.

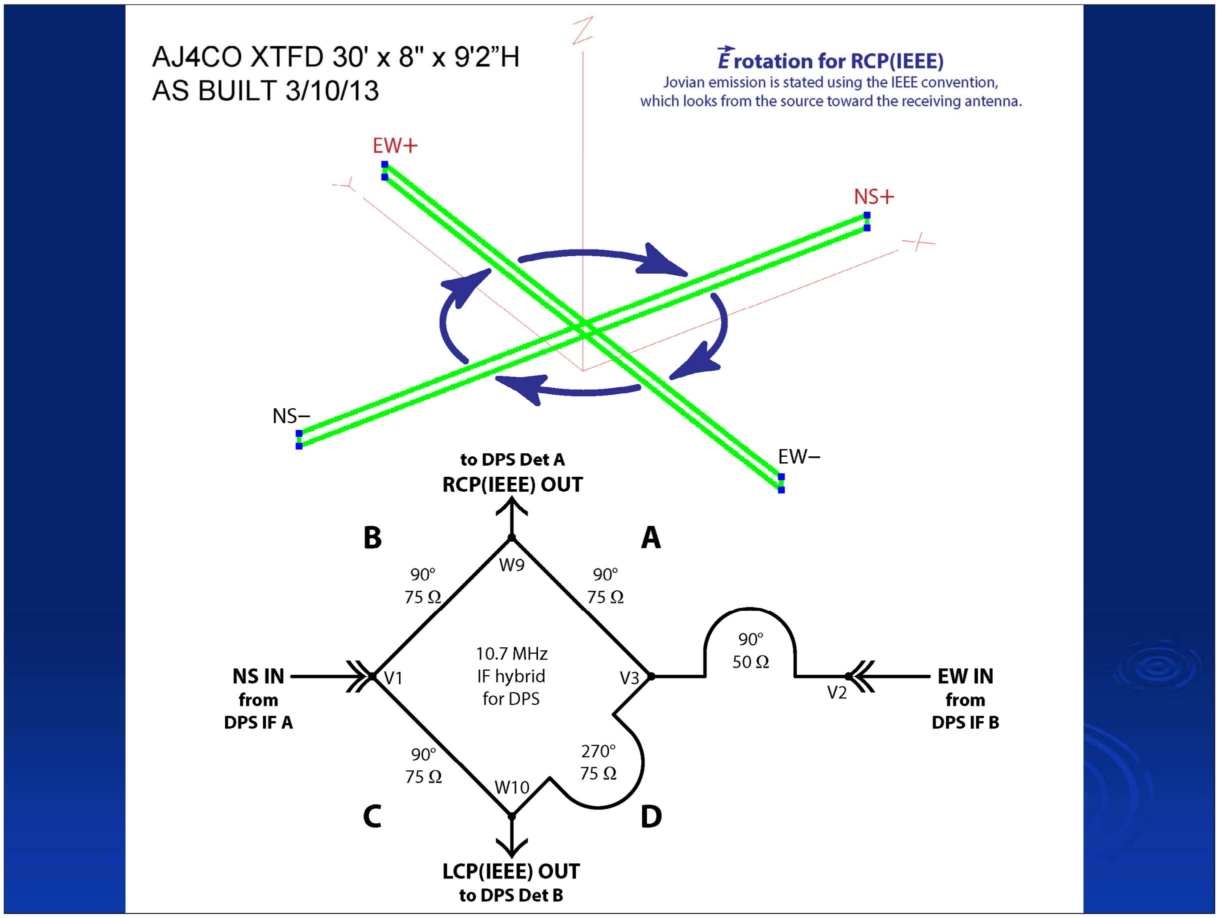

The DPS doesn't *have* to be used for RCP and LCP – it can accept any two RF inputs and record correlated samples. We have used RCP and LCP because that seems the most useful option.

Circular polarization was discussed in the Advanced Systems talk. The important point for us is describing how the E field vector rotates in the plane of the antenna array aver time. In the picture above, we see two orthogonal dipole antennas forming an array. The IEEE definition, which is what radio astronomy uses, says that if the E vector rotates clockwise in the plane of the array as viewed from the source, the emission is right circular polarized (RCP). If it rotates counterclockwise, it's left circular polarized (LCP).

Shown above is one method of extracting circular polarization from orthogonal antenna elements: by using a 180° hybrid ring, which is just several pieces of coax of appropriate length and impedance connected together. This hybrid can be inserted between the DPS's IF outputs and the detectors. This is an easy way of seeing how CP can be generated. The signals at this point in the DPS are all at 10.7 MHz, so a wide bandwidth hybrid is not required.

To see how this works, simply follow the phase delays. For RCP, the positive end of the EW dipole leads the positive end of the NS dipole by 90°. When these two signals enter the circuit shown on the bottom of the image, the EW signal is delayed 90°. So, at the inputs to the hybrid ring itself, RCP signals are in phase. Adding 90° to both leaves them still in phase at the RCP ring output. But adding 90° to one and 270° to the other leaves them 180° out of phase at the LCP output, so they cancel.

The opposite holds true if we reverse the direction of the circular polarization and follow an LCP signal through the circuit.

A picture of the hybrid ring is shown on the next page.

This configuration was used for several months. When it became desirable to also use two Jove receivers to form a polarimeter by measuring RCP and LCP at two closely spaced frequencies, this setup had to be abandoned – that is, we needed a way to generate CP before the mlticouplers, not just inside the DPS itself. A second method of generating CP is now used, placing a wideband 90° hybrid at the inputs to the multicouplers (see slide # 6, Antenna Entrance Panel diagram). The wideband 90° hybrid separates RCP and LCP by a rather complex process that your author does not even pretend to understand. This second method has the benefit of making RCP and LCP available for other receivers in addition to the DPS.

The TFD Array

The DPS is a nice instrument and we felt it warranted an equally nice antenna array. The desire was for and array that would have a wide bandwidth, decent gain, and low cost. The TFD array evolved from some experiments with single and crossed TFD elements into a dual-square, 8-element array.


DATE: 22 OCT 2013
SCALE: 1 mm = 1 ft
AJ4CO
OBSERVATORY
TFD Array
SOUTH
26.9°

TFD Array Element

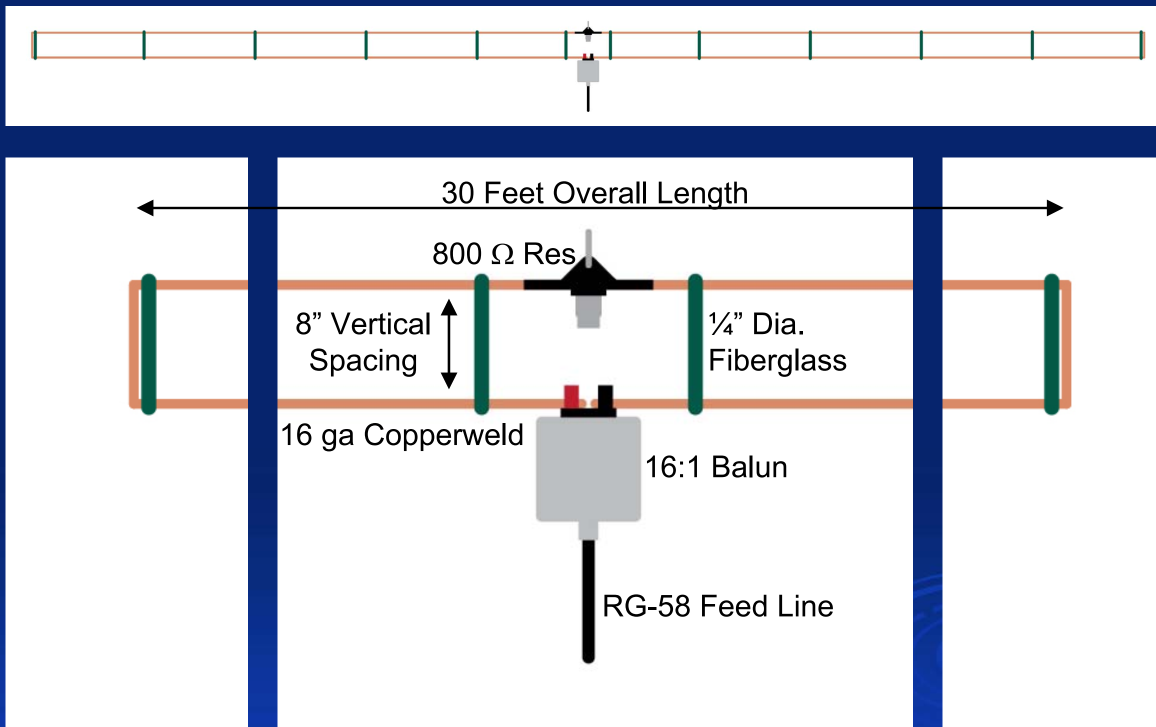

A diagram of a terminated folded dipole (TFD) element.

Each TFD element is 30 feet wide with a wire spacing of 8 inches. The element has an 800 ohm terminating resistor in the center at the top and a 16:1 balun transformer in the center at the bottom.

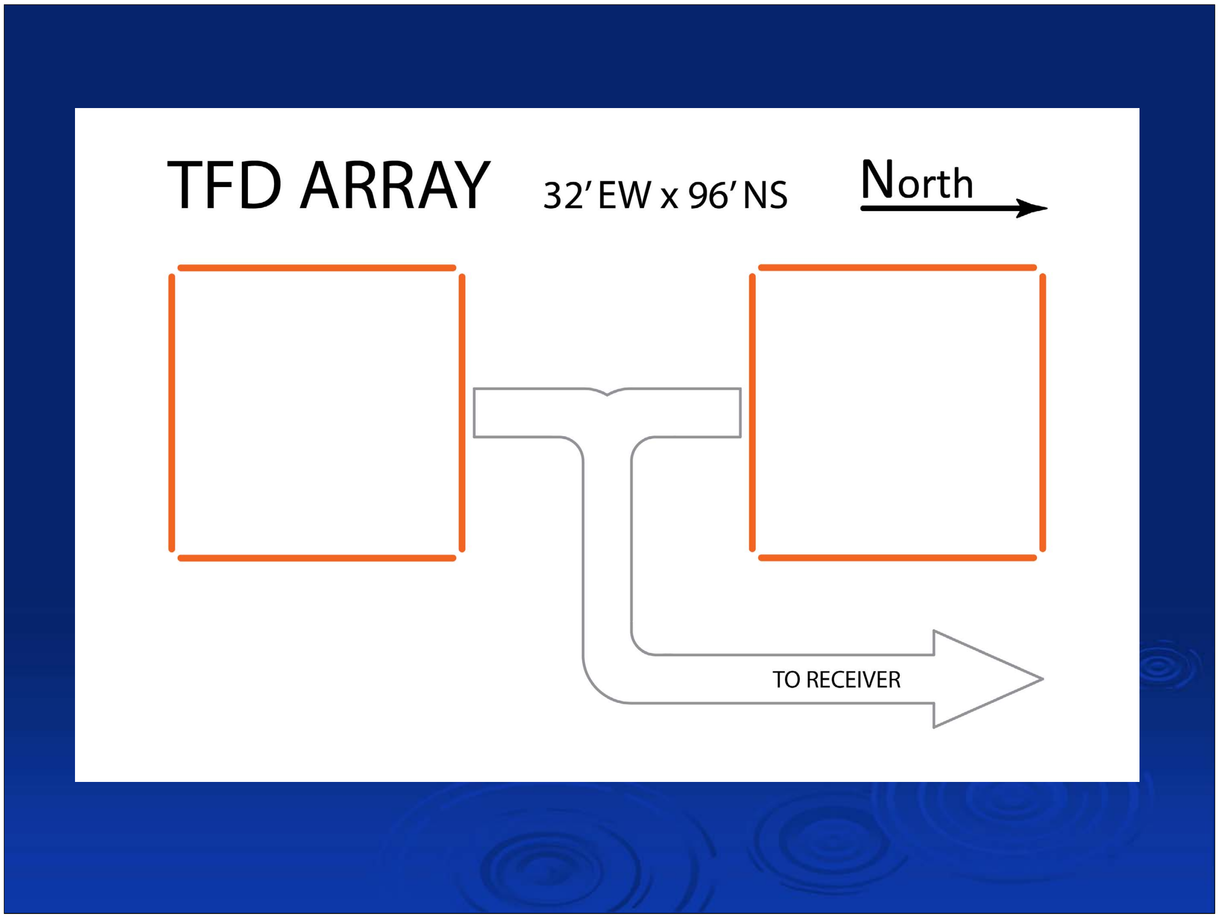

Here is a diagram of the 8-element TFD array. Two squares, each 32 by 32 feet, separated from each other by 32 feet.

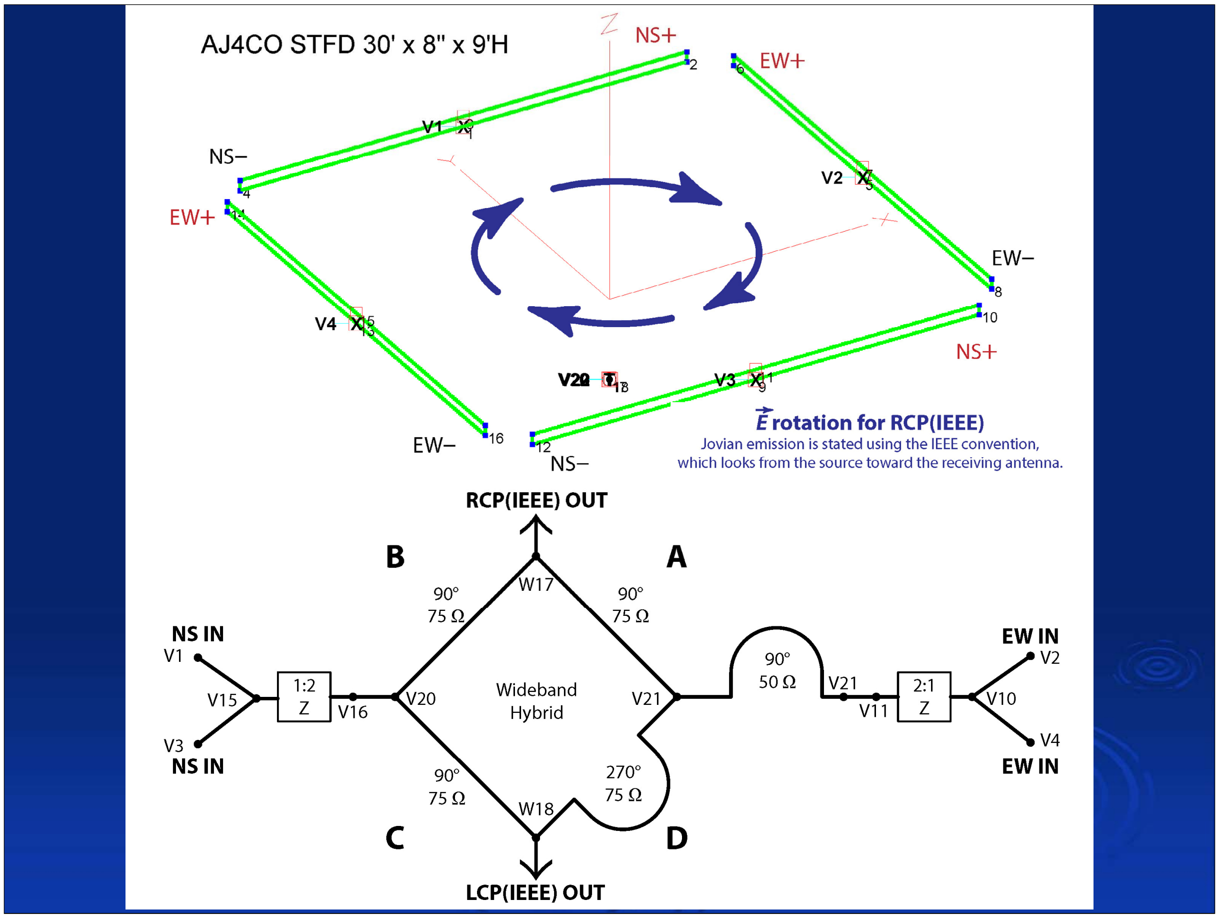

One "square" of the TFD array. A square is just an expanded cross (slide #9); the separation of RCP and LCP works the same. The curved arrows in the diagram only show the rotation of the emission's electric field vector for RCP; they do **NOT** show the instantaneous polarity of each element in the square array. For example, when the E vector is pointing east, **BOTH** east-west elements see the E vector pointing east – that is, they see the same signal, in phase.

The diagram shown below the antenna wires represents the transmission lines in the EZNEC model, including impedance transformers (not present in the actual antenna, but required in the model to keep the impedances correct) and the wire and virtual wire segments (the "W" and "V" numbers) that act as junctions.

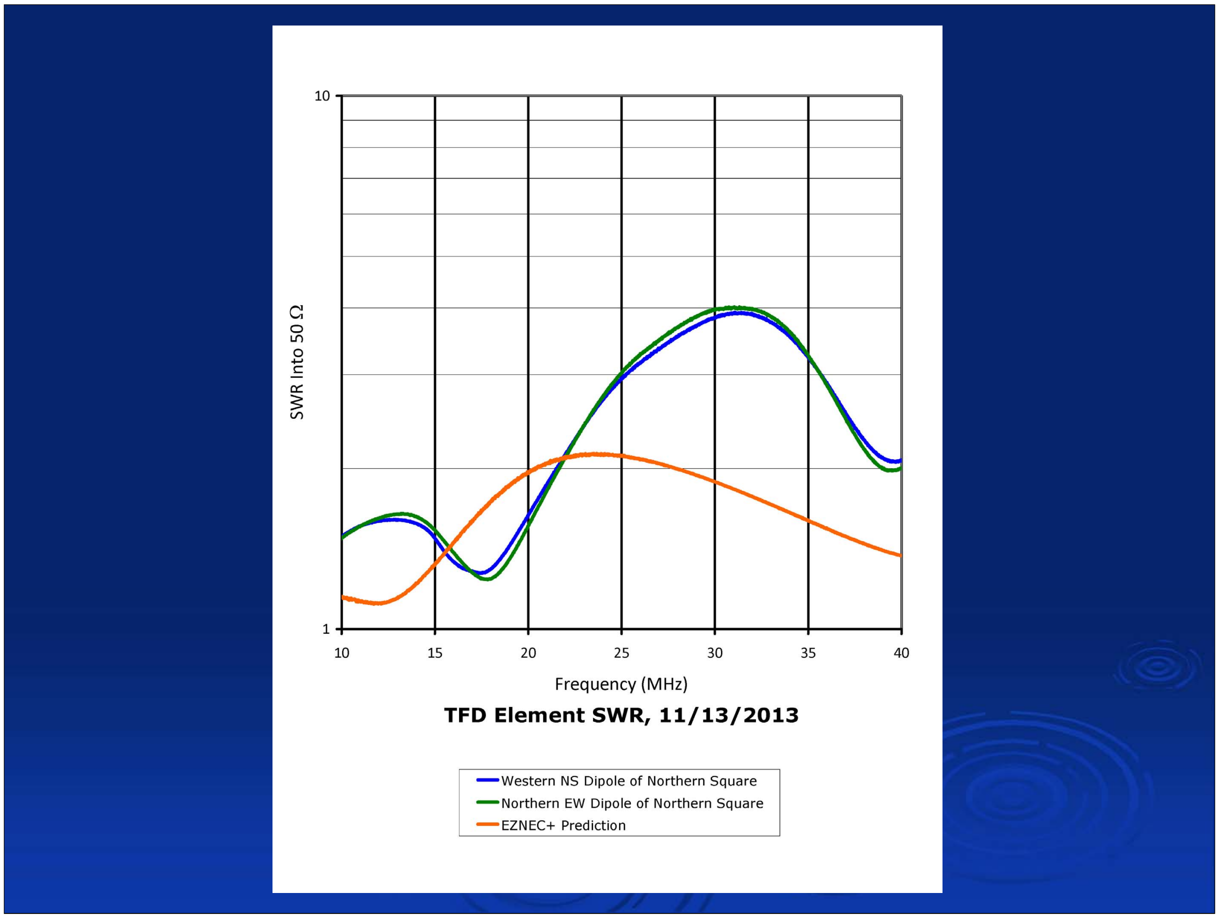

SWR sweeps performed with a VNA-2180 on two different single TFD elements (green & blue) at their balun outputs as installed in the 8-element array, compared to the EZNEC prediction for a single TFD element (orange) by itself over ground.

The loss associated with an SWR of 4:1 is 2 dB. As such, the TFD array produces a "built-in" loss curve that goes from 0.08 dB loss at 16 MHz to 2 dB at 32 MHz in a relatively straight line. The effect of the loss curve could be removed during post-processing of the spectrograph data; this is a planned future enhancement to the RSS software.

The SWR acts to reduce the maximum gain of the antenna without changing the directivity. That is, the SWR reduces all the signal power equally in all directions. An outstanding explanation of the difference between gain and directivity is available here: Smith and Carr, "Radio Exploration of the Planetary System", Van Nostrand (1964) pp. 13-16. < **https://archive.org/details/RadioExplorationOfThePlanetarySystem** >

TFD Array Construction

The 16 ga Copperweld element wires have an 8” spacing maintained by cross-drilled fiberglass rods. A short U-shaped loop of 22 ga copper is soldered around the rod to keep the rod from sliding along the Copperweld. This is one of a series of six toggle clamps used to position the rods during element construction.

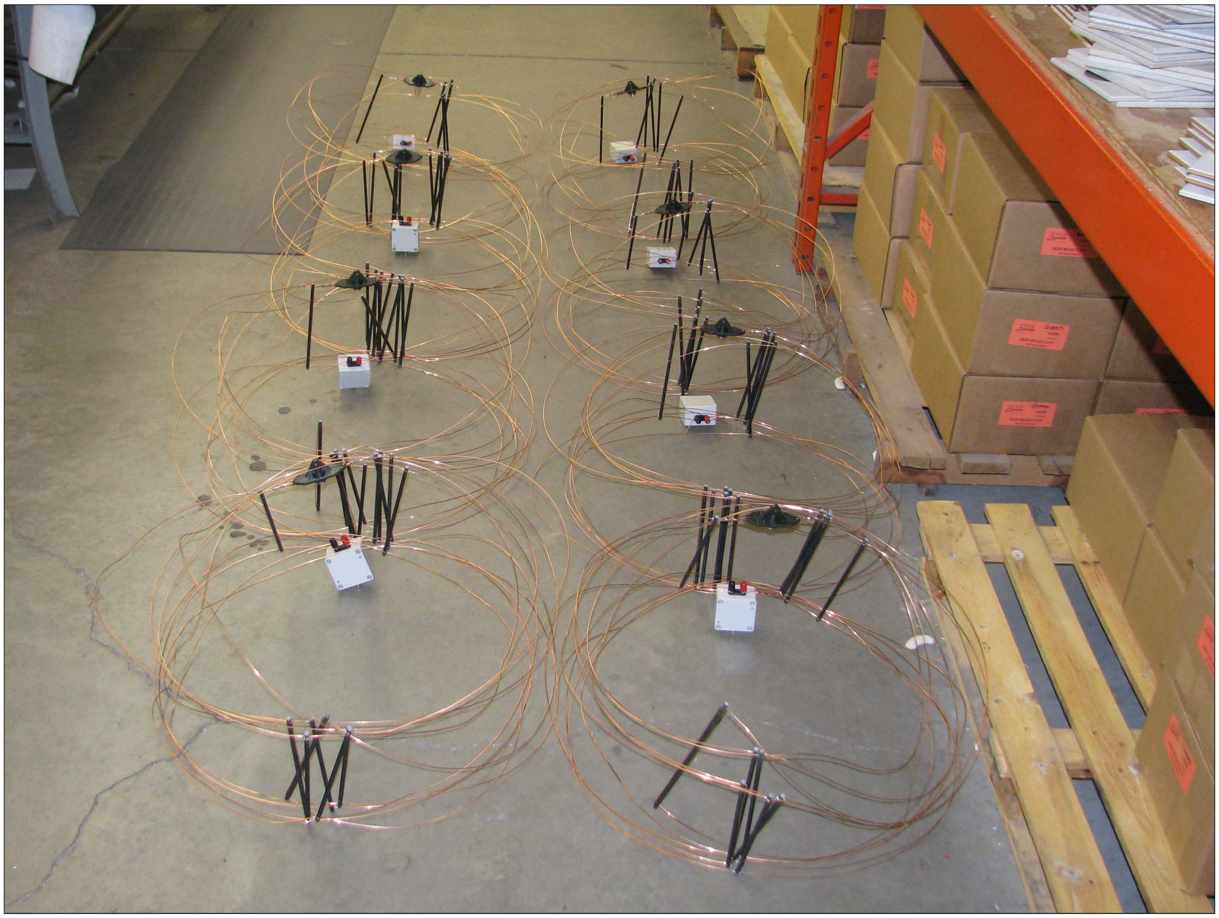

Eight TFD elements ready for installation. This represents 500 feet of 16 ga Copperweld (about 62 feet per element).

View of the TFD array, looking north and slightly west.

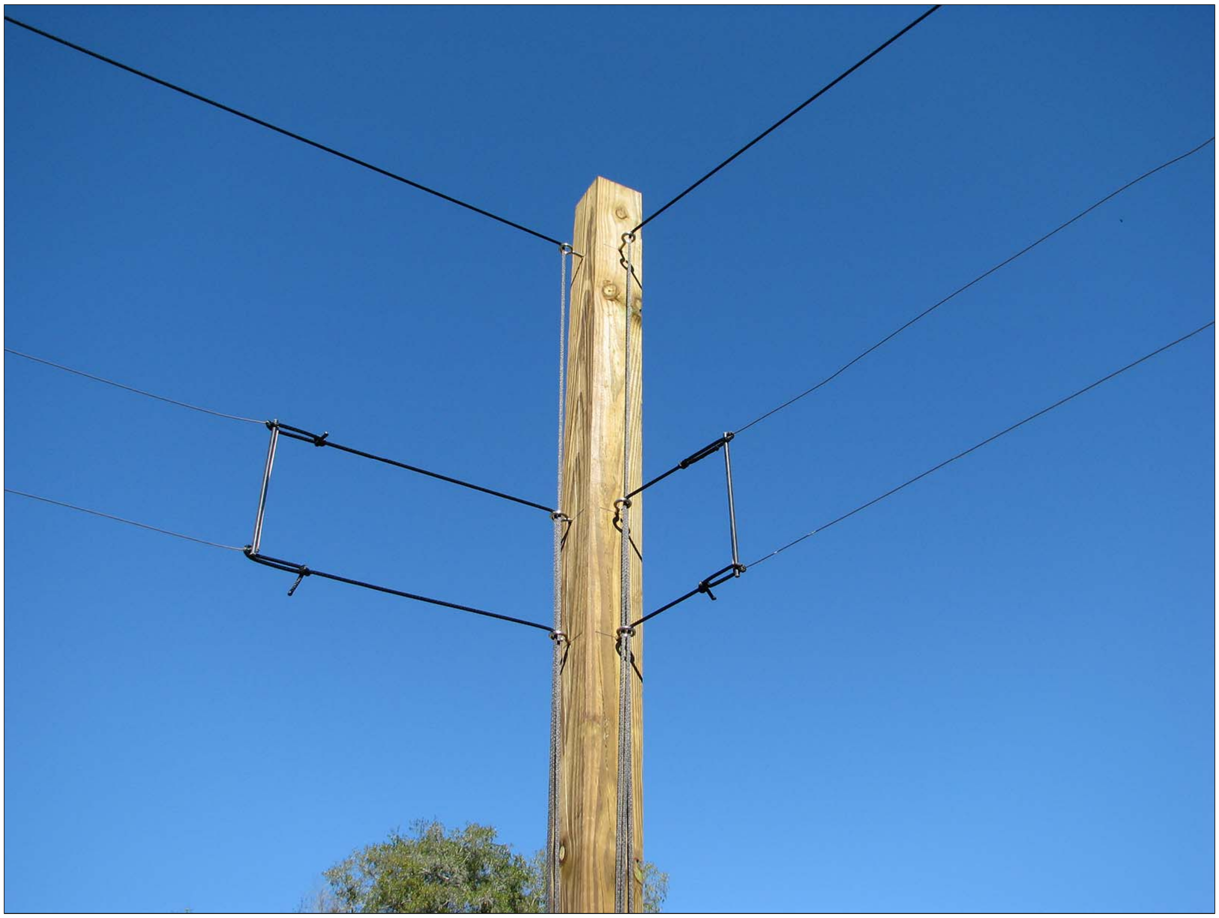

3/16” black polyester rope serve as halyards, running through stainless steel screw eyes. There is about 500’ of rope in the array.

Cleats hold the lower ends of all the halyards.

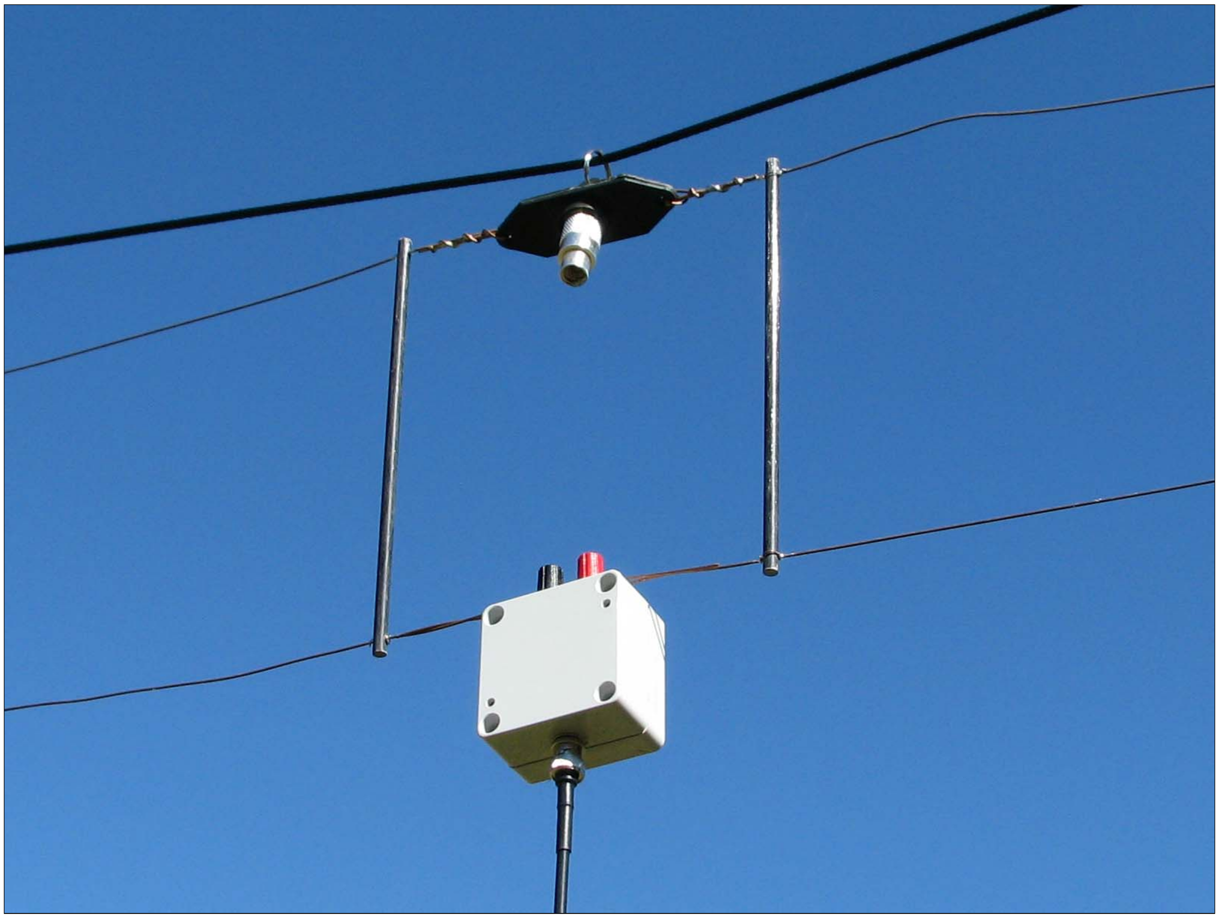

A Budwig center insulator allows for a center support rope to hold up the middle of the element. It is also the attachment point for the 800 ohm non-inductive terminating resistor, which is soldered inside a PL-259 coax connector.

The gray box is the 16:1 balun transformer.

16:1 Balun Transformer

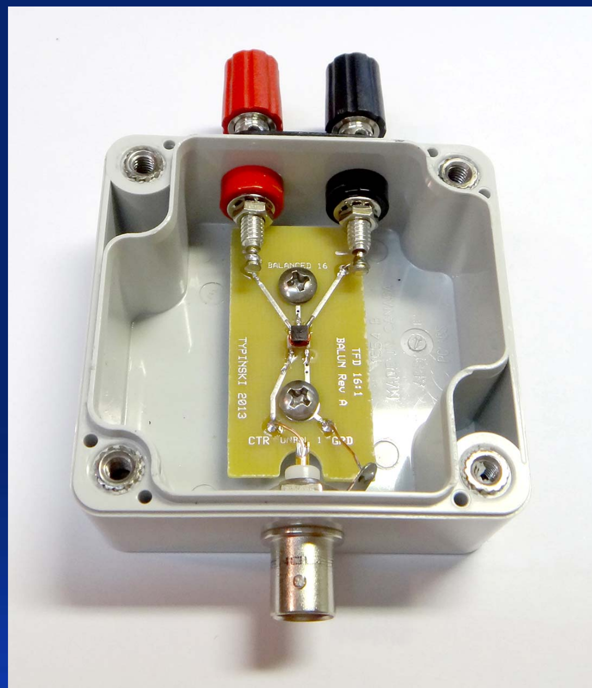

The balun is custom designed and built around a Mini-Circuits TC16-161TX+ 16:1 SMD balun transformer. The unit is rated at 250 mW; so far, lightning spikes have not damaged any of the TFD's baluns.

TFD Balun Measurements

Insertion Loss SWR

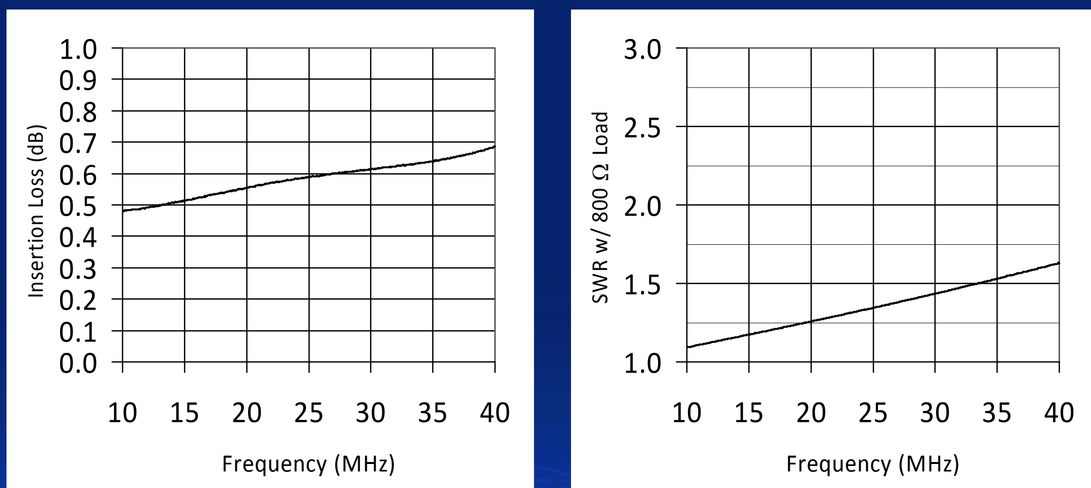

The balun's performance was measured with a VNA-2180.

LEFT: **insertion loss**, measured by putting two TFD baluns back to back and dividing the measured loss by two.

RIGHT: **SWR**, measured by using an 800 ohm non-inductive resistor in place of the antenna.

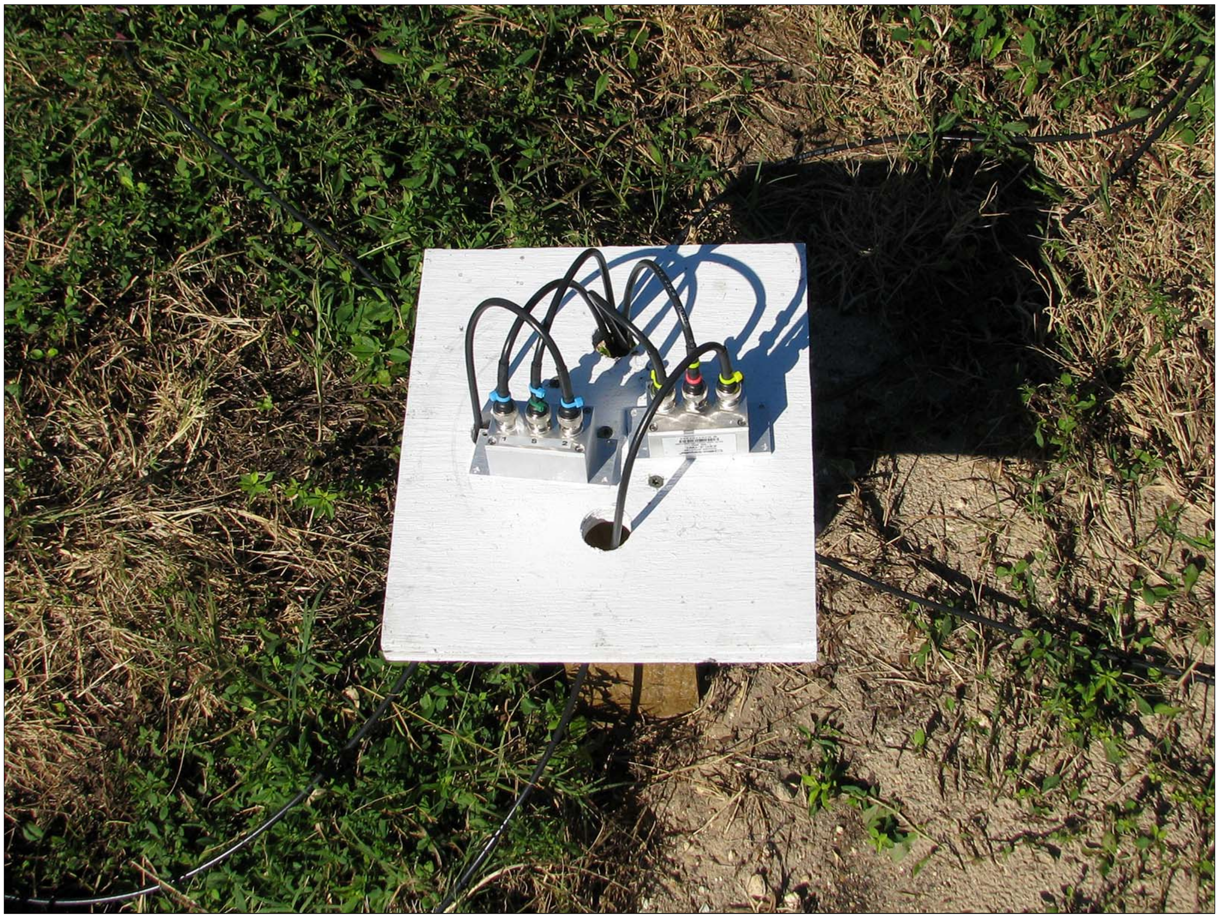

Here is the inside of one of the three junctions boxes used in the TFD array. This one contains the two power combiners that bring signals from the two squares together, for transmission to the receivers. There are no delay cables installed in this picture, so the beam was pointing at zenith.

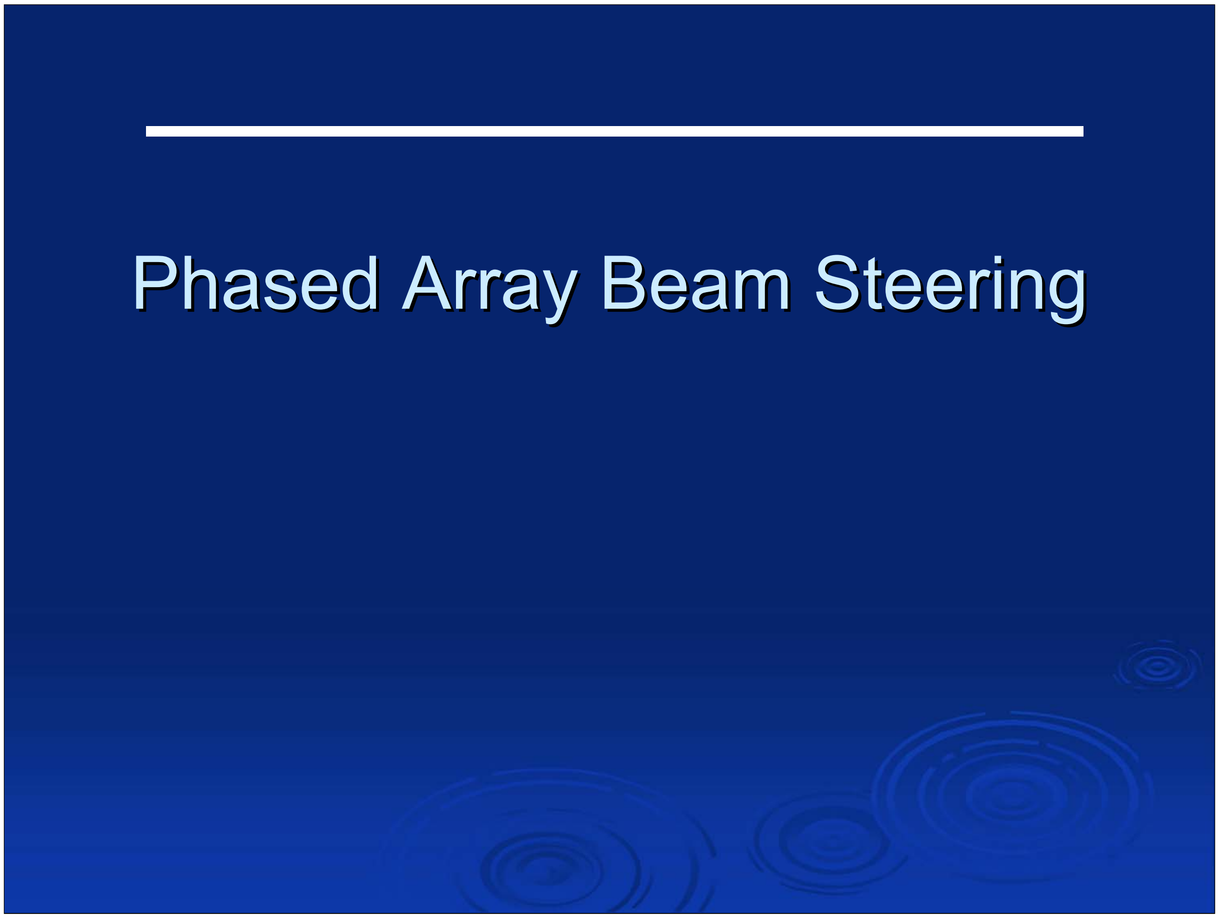

Now we must talk for a bit about how to point all these TFD elements at a spot in the sky – and what happens when you actually do that.

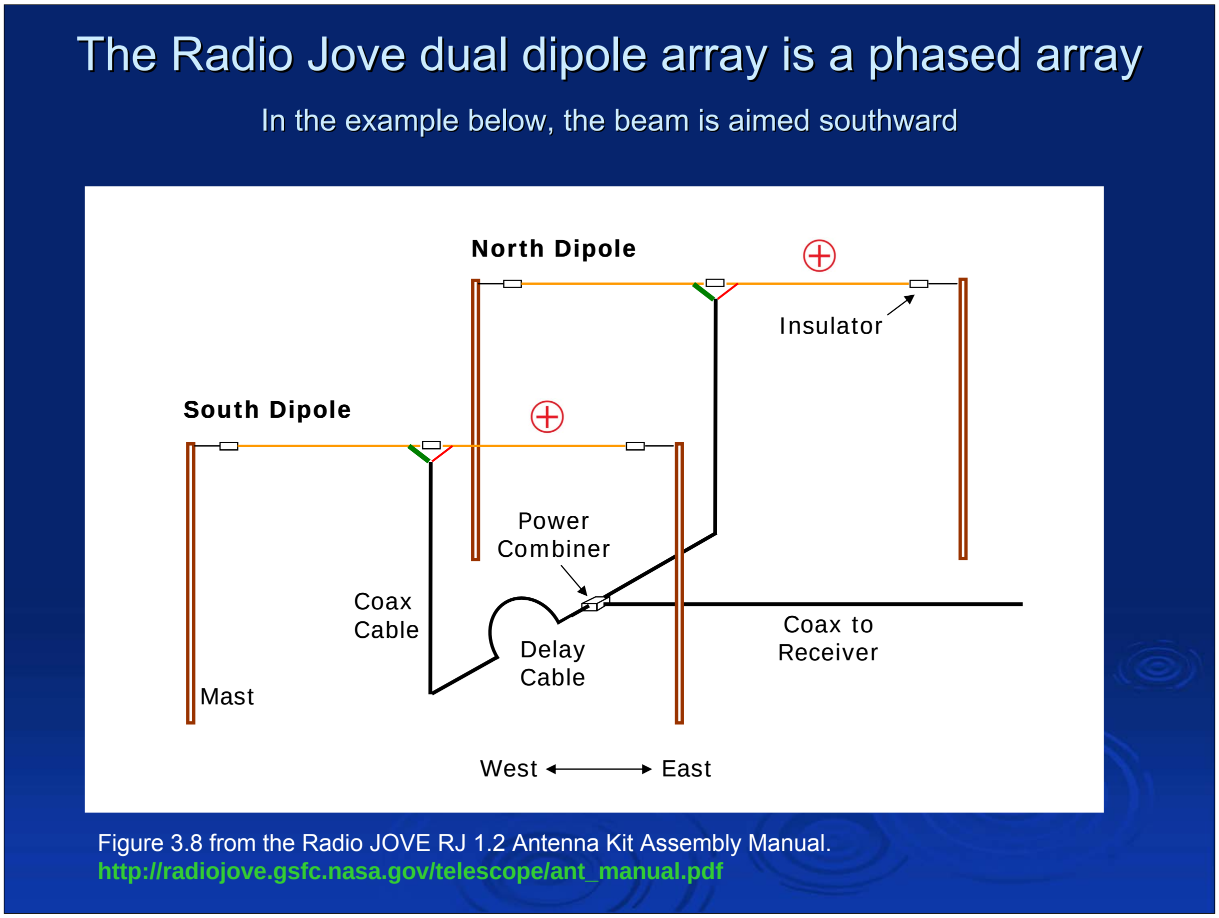

Figure 3.8 (slightly modified) from the Radio JOVE RJ 1.2 Antenna Kit Assembly Manual.
http://radiojove.gsfc.nasa.gov/telescope/ant_manual.pdf

The Jove manual specifies the delay cable in terms of degrees of phase at 20.1 MHz. For example, if the southern dipole is to be delayed by a quarter cycle at 20.1 MHz, we simply add a 90° phase cable to it’s feed line. This works great since an array of half wave dipoles is not a wideband antenna.

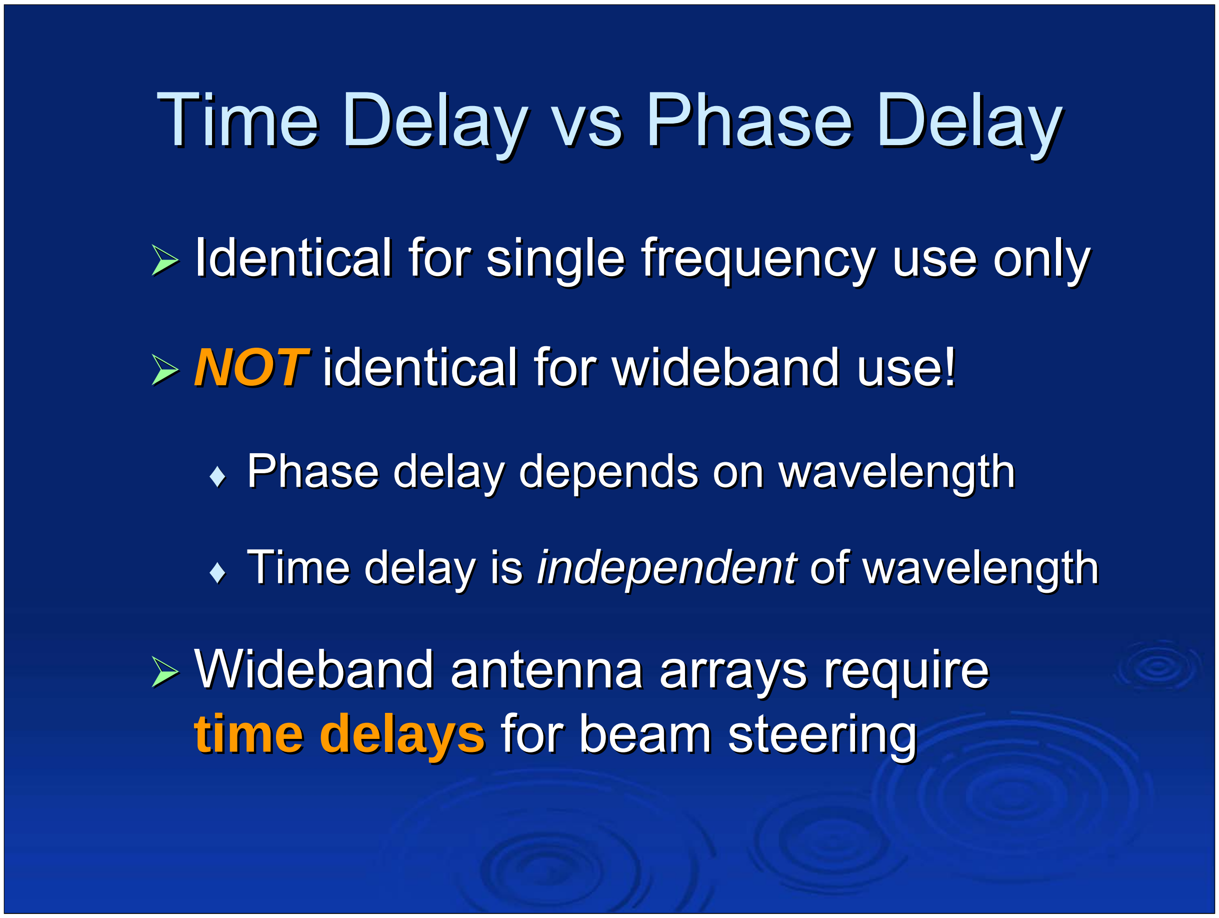

To calculate the required length of a delay cable, we have two choices. We can work in terms of time delays or in terms of phase delays.

For wideband antennas, it is necessary to work in terms of time delays because **phase relationships change with frequency while time delays do not**. This is readily apparent in the three simple equations on the next slide. The equations also show that it is also easier to work in terms of time delays since time delay calculations are simpler than phase delay calculations.

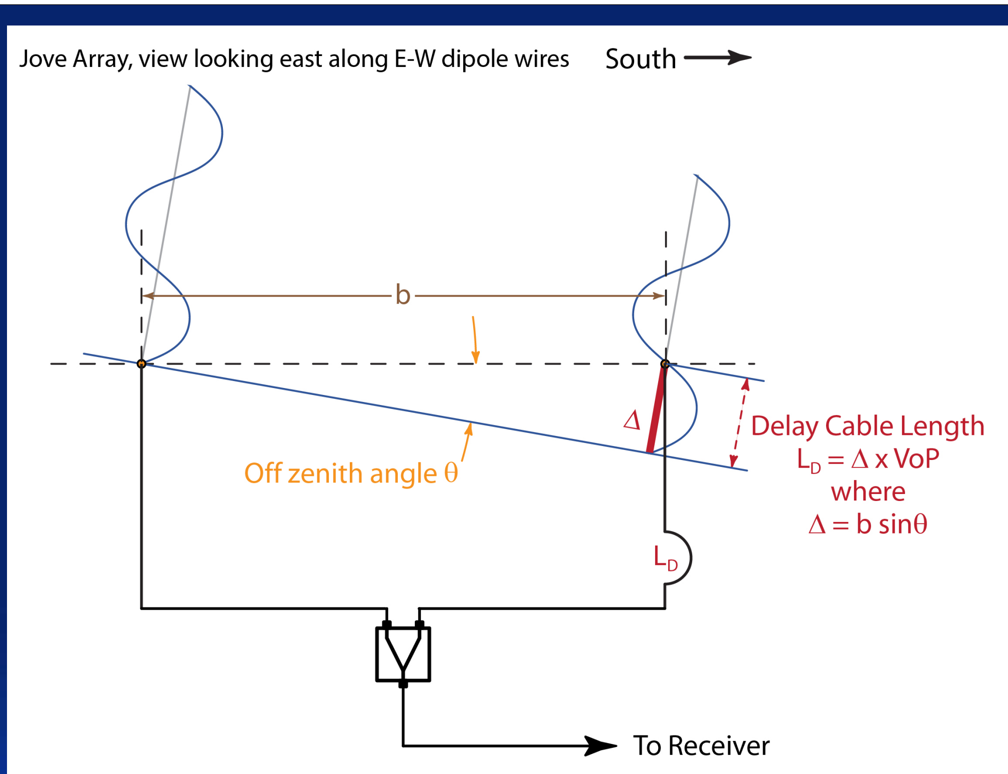

$$\text{Delay Cable Length} = \Delta(\text{VoP}) = b \sin\theta(\text{VoP})$$

Here is an example of a simple phased array, the Jove array.

For any phased array, the idea is to combine the signals from each element while making sure that the signals are in phase **at the receiver input**.

If the source is directly overhead, it's easy: the signals at each element are in phase, so we can use equal lengths of feed line between the elements and the power combiner.

If the source is not at zenith – say, slightly south of zenith – then the signals at each element are not in phase – the northern element's signal is delayed. That is, if we imagine a plane wave coming from a point south of zenith, then the wavefront will contact the southern element before it contacts the northern element.

We can force the signals to be in phase at the receiver input by introducing a delay to the southern element's signal; we do this by adding an appropriate length of coax to the southern element's feed line. The appropriate length is simply delta times the velocity of propagation (VoP) in the coax. Delta is found very easily with plane trigonometry. VoP depends on the type of coax; it is stated on the manufacturer's data sheet and is usually somewhere between 65% and 85%.

EXAMPLE: if Jupiter has an elevation of 70° at meridian crossing, then we wish to steer the beam 90°-70° = 20° south of zenith. To do this, we install a delay cable on the southern element of the Jove array. Let's assume we will use RG-58 or RG-59 coax, both of which have a VoP of 66%. In the Jove array, the distance b between the elements is 20 feet.

The required delay cable length will be 20' sin(20°) x 66% = 4'6". Note that this is independent of operating frequency.

Note that whether the wave travels through air or coax, a delay is a delay. To steer the beam, we're just swapping a delay in air for a delay in coax. In other words, we could steer the beam by physically tilting the array to add some delay to the southern element – but that's much more difficult than installing a delay cable.

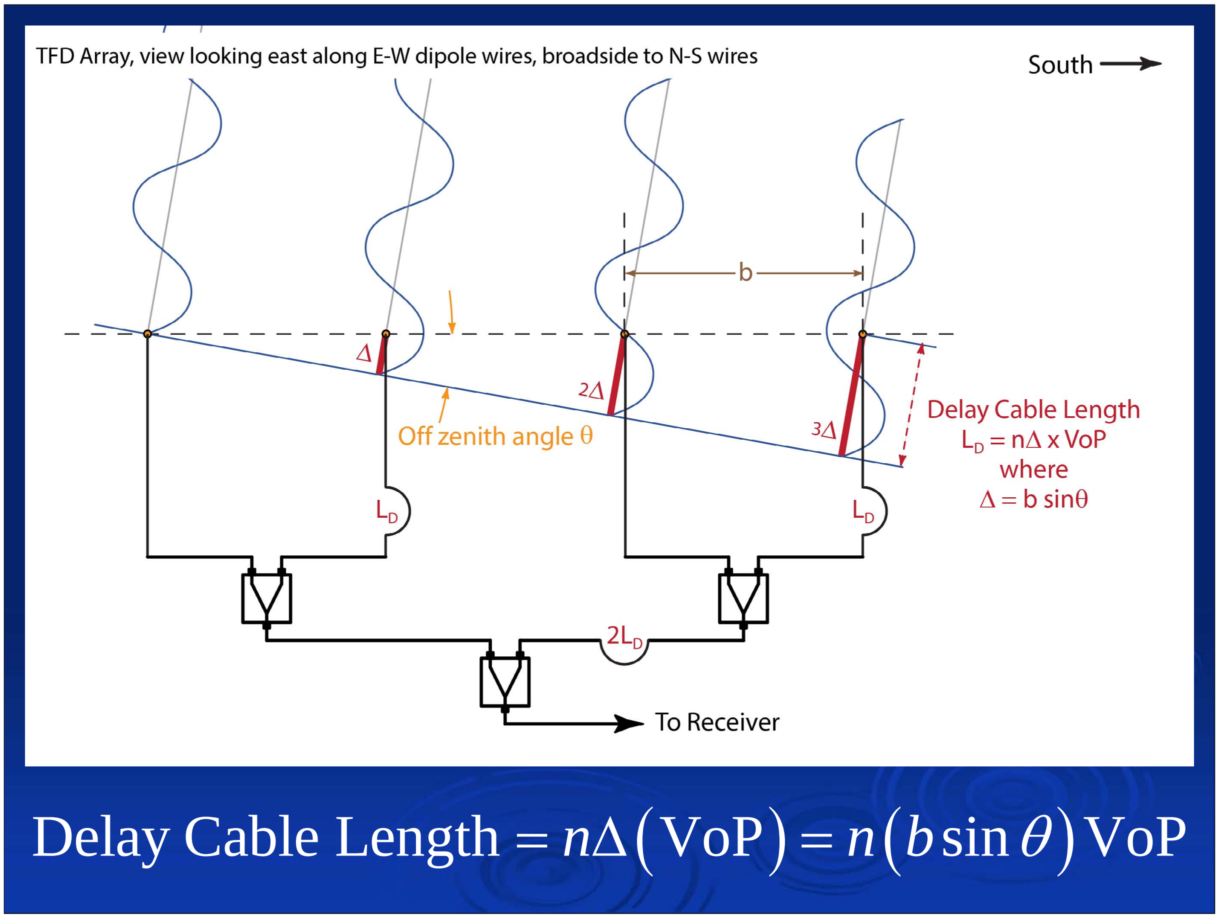

Here is an example of an array with more elements. The process is exactly the same as described on the previous slide, just with multiple delay cables.

Note that what matters is the phase delay applied to each element's signal before it reaches the receiver input. Trace out the total phase delays applied to each element's signal and we see that they in fact progress from 0, 1, 2, and 3 multiples of the basic delay.

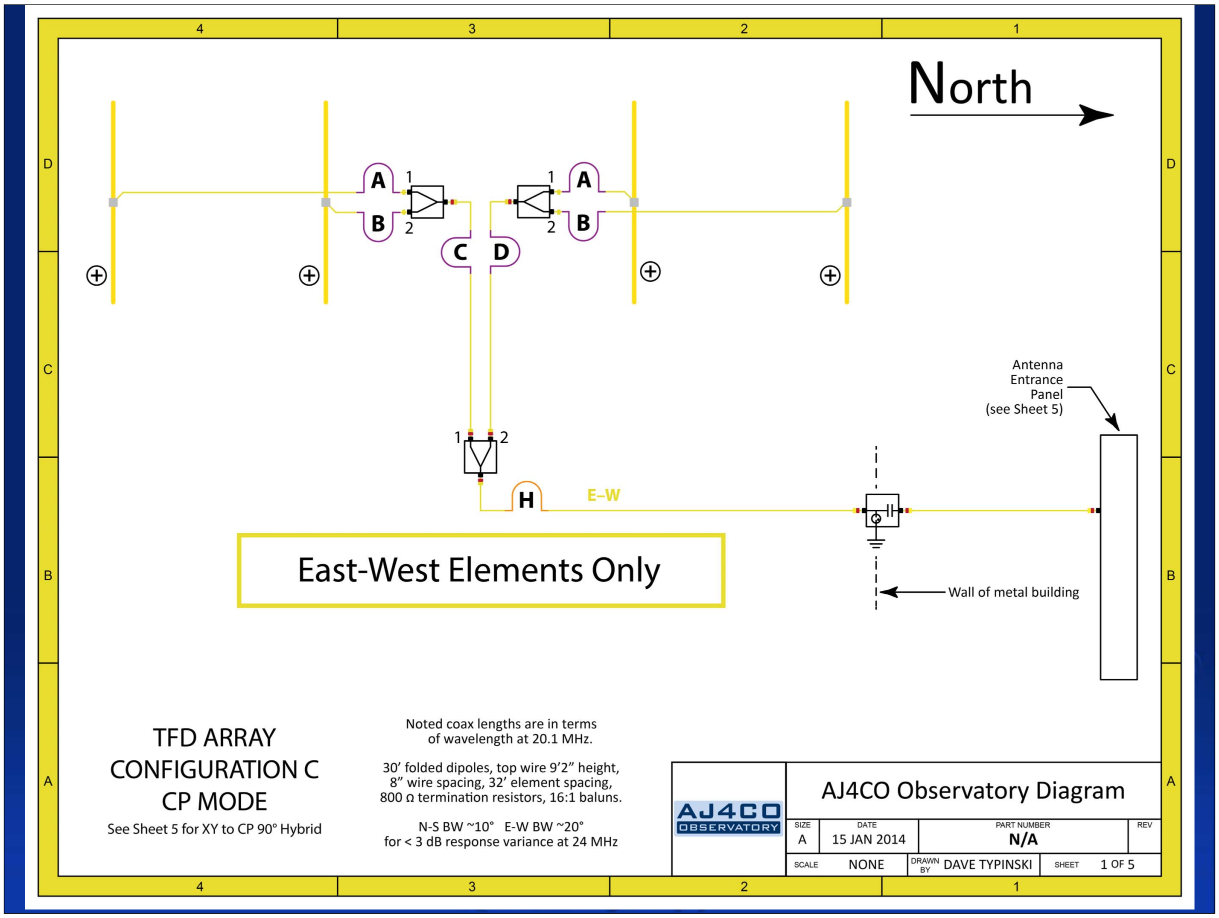

The TFD array is really a combination of two arrays. This is one: all the east-west elements. This diagram shows the associated delay cable positions. Varying the length of these delay cables steers the beam north and south.

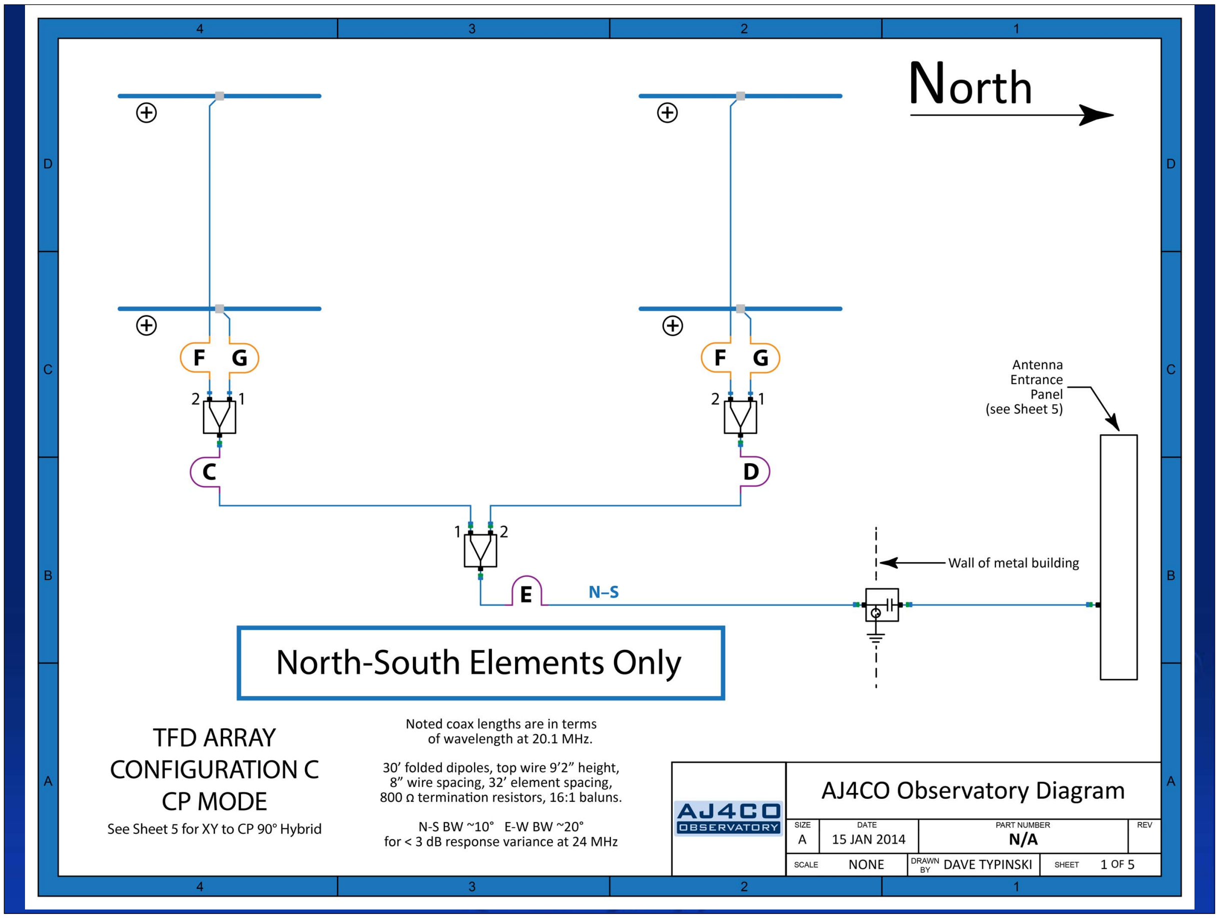

The other is all the north-south elements. This diagram shows the associated delay cable positions. Varying the length of the ORANGE delay cables steers the beam east and west. Varying the length of the PURPLE delay cables steers the beam north and south.

Simple beam steering, however, does not tell the whole story!

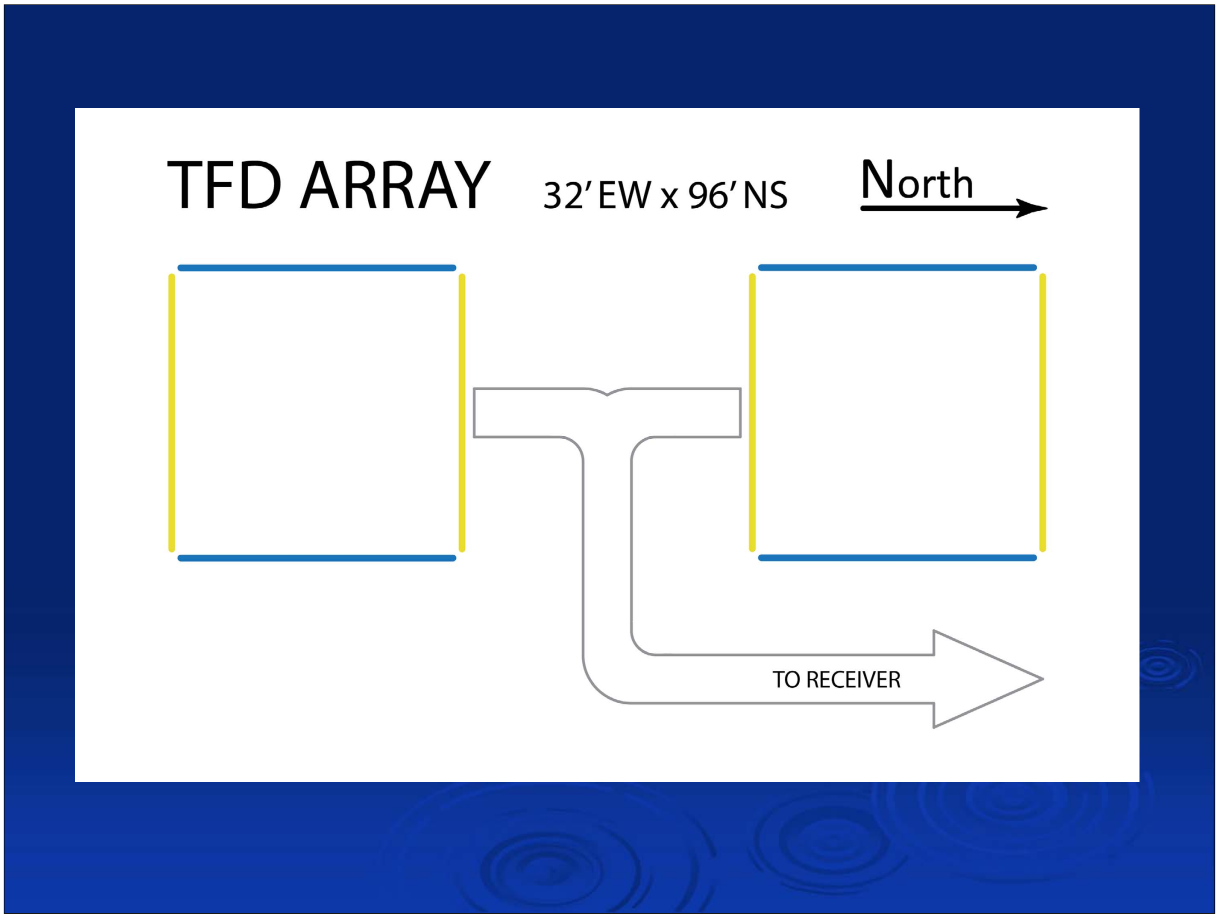

Since the TFD array is a combination of the yellow and blue portions, simple beam steering, however, does not tell the whole story! To see where the beam of the whole array is pointing, we have to analyze the pattern of a TFD element, the pattern formed by an array, and the combinations they form.

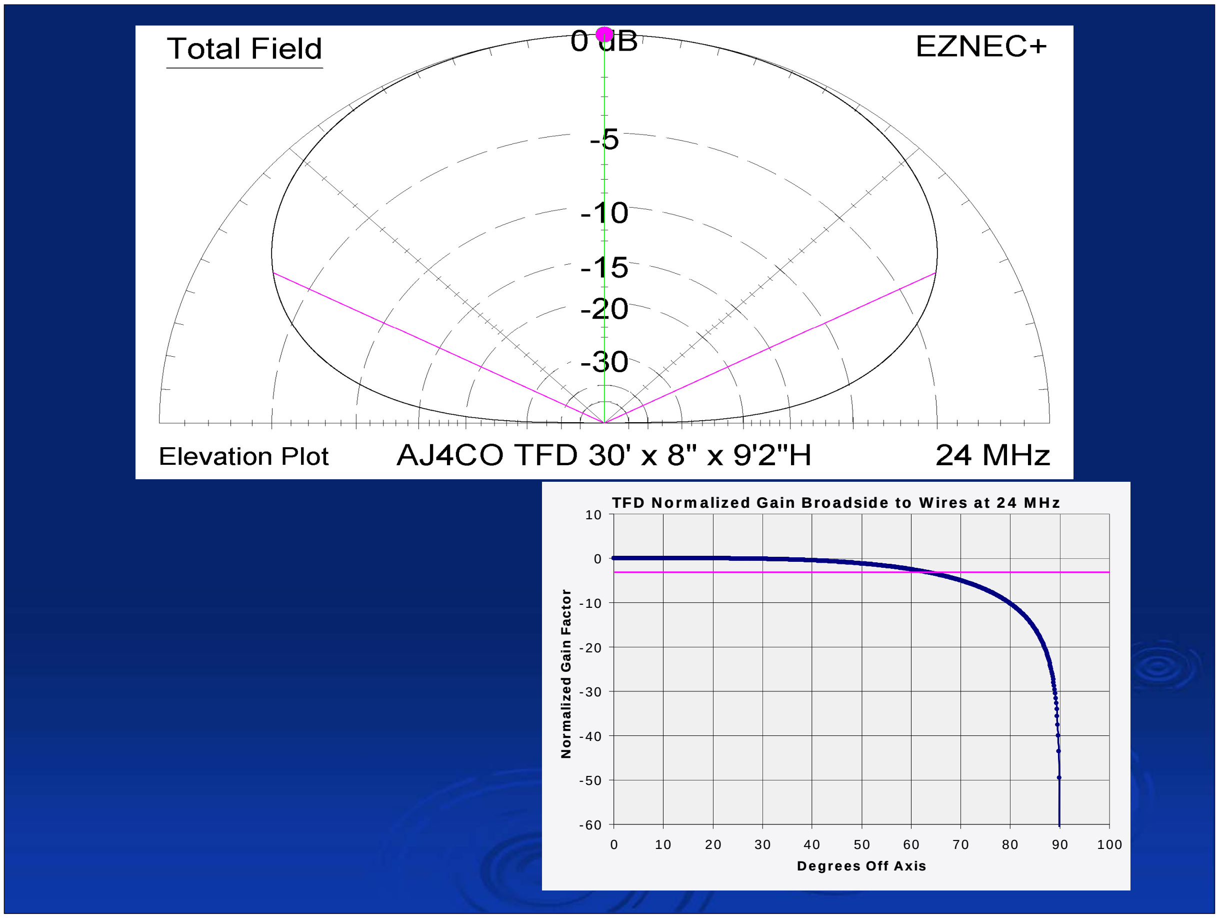

Here are two ways to plot elevation pattern data.

TOP: a polar plot showing an elevation slice of the antenna beam. Radial scale is in dB down from peak gain at zenith.

BOTTOM: a rectangular plot showing the same data, but only from zenith to on horizon. Vertical scale is in dB down from peak gain at zenith.

Since the TFD element is physically symmetric in the broadside direction, only half of the elevation data needs to be plotted – the "left hand" half of the top plot is simply a mirror image of the "right hand" half.

NOTE: in both plots, the half power point is at 62° from zenith (pink lines in both plots).

We can plot the response of a TFD element at several frequencies and in two directions (broadside and in-plane-of-wires) using rectangular plots.

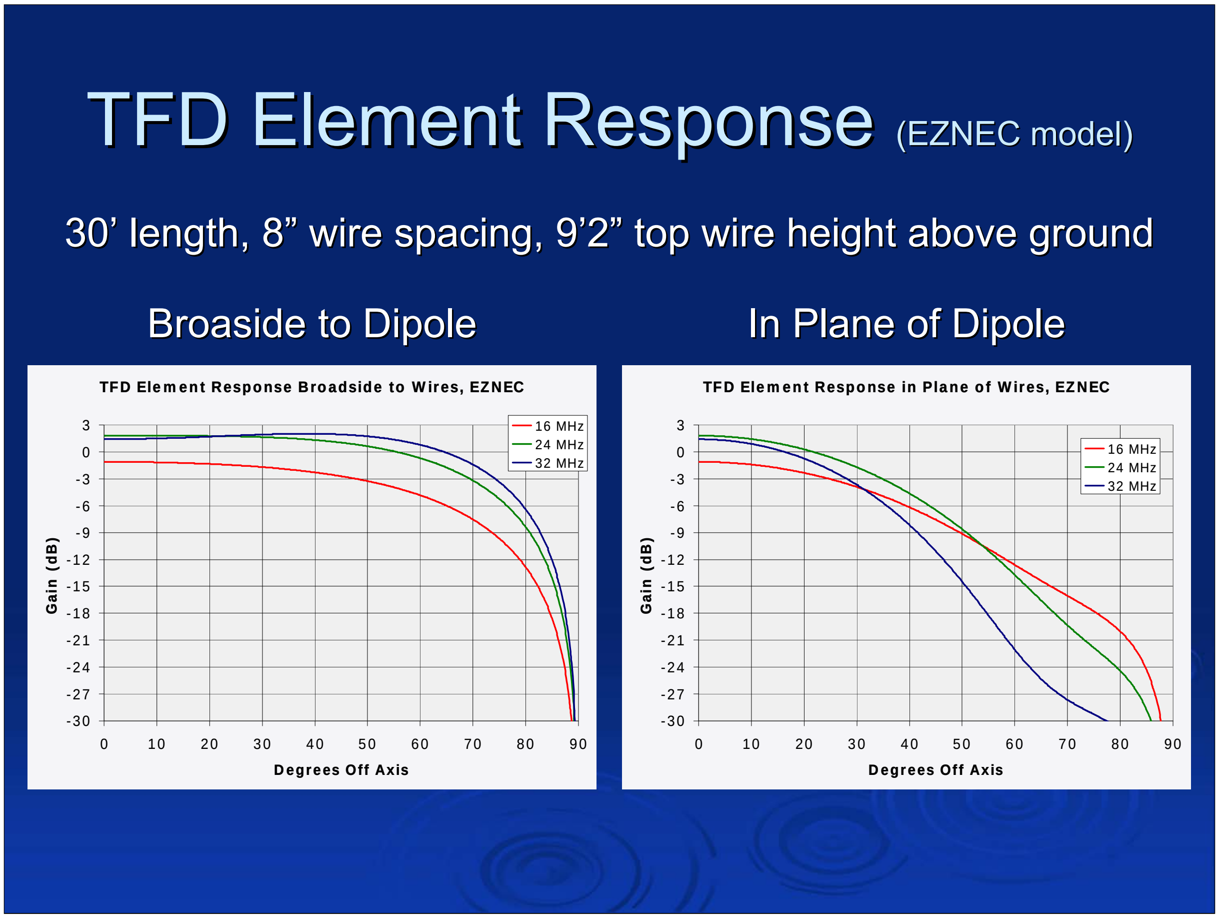

Here are rectangular plots of one TFD element's response (elevation patterns) in two directions: in the plane broadside to the element's wires and in the plane of the element's wires. Plot traces represent the elevation patterns at 16, 24, and 32 MHz.

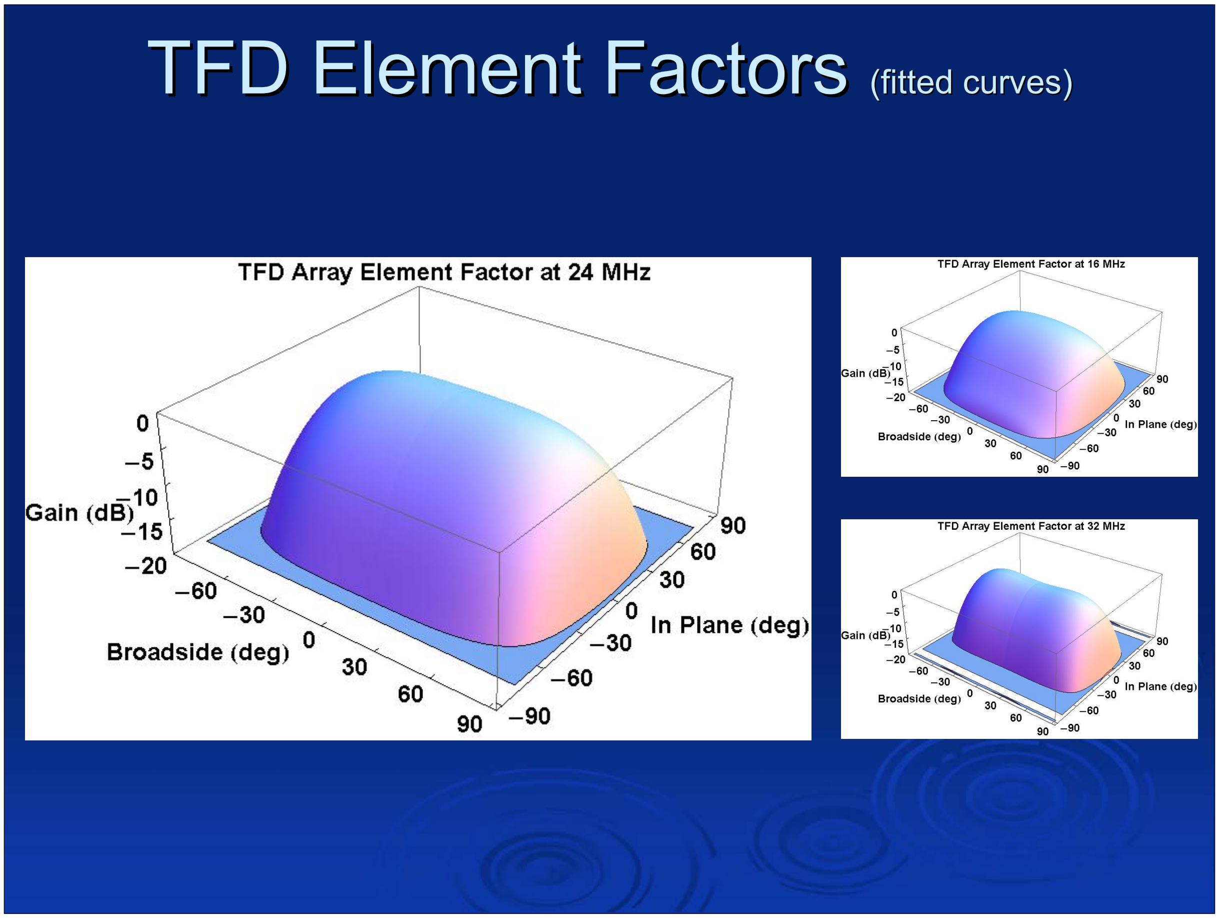

We can take the data plotted in the previous slide and fit some curves to it, then plot those curves in three dimensions to arrive at some mathematical functions that represent the element's beam shape.

6th order polynomials were fitted to the curves shown on the preceding slide. When plotted in three dimensions, this is the result: one TFD element's pattern at three frequencies. But instead of a table of values, we now have mathematical functions that can be used the calculate the response of the whole array.

These mathematical functions are called "element factors" – factors, because they're multiplied with the "array factors" (see next two slides) to obtain the response of the array as a whole.

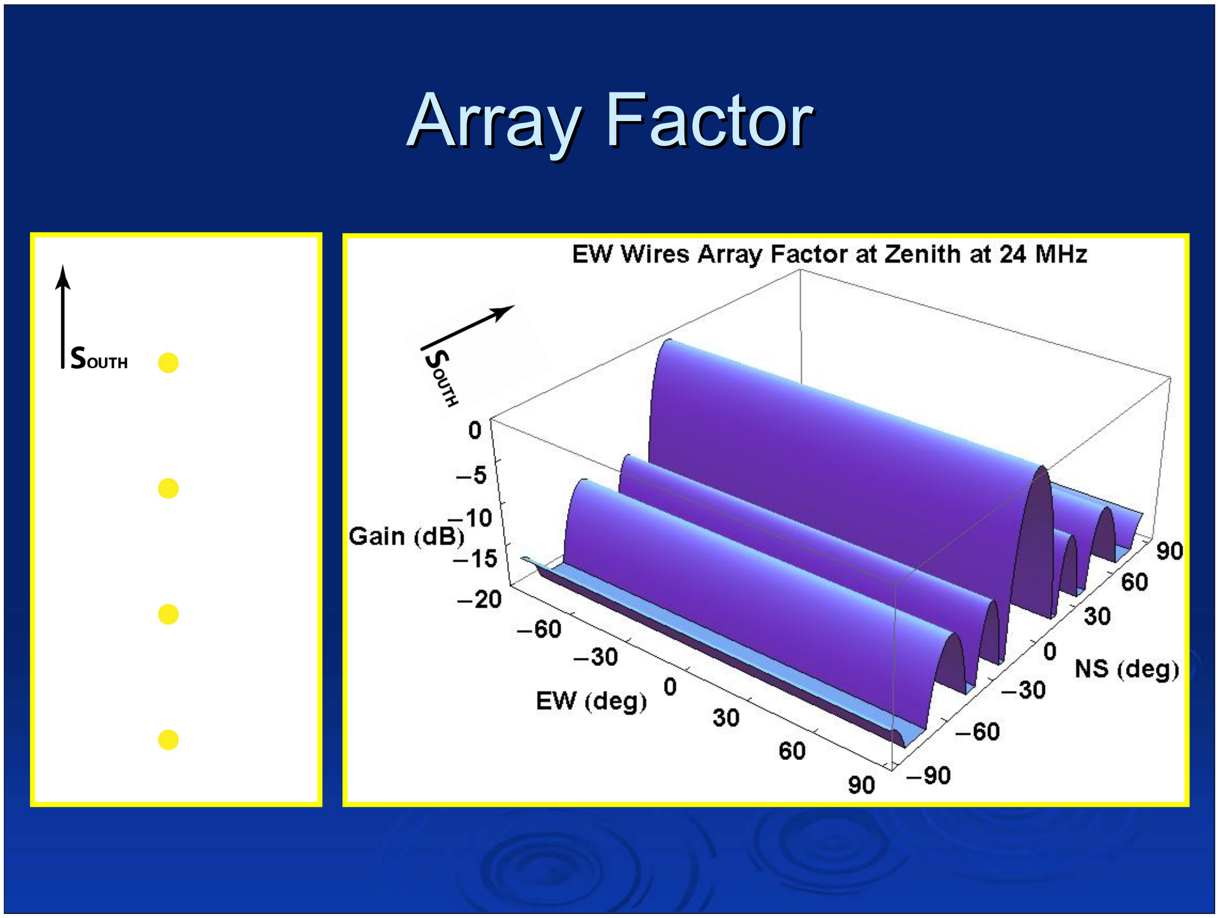

An array factor is the beam one would get by replacing the real array elements with **isotropic radiators**. Since isotropic radiators receive equally well from all directions, calculation of the beam is relatively easy (see slide # 46) – it is simply an interference pattern.

The reason we want to find the array factors is that it makes calculation of the array beam shape easier.

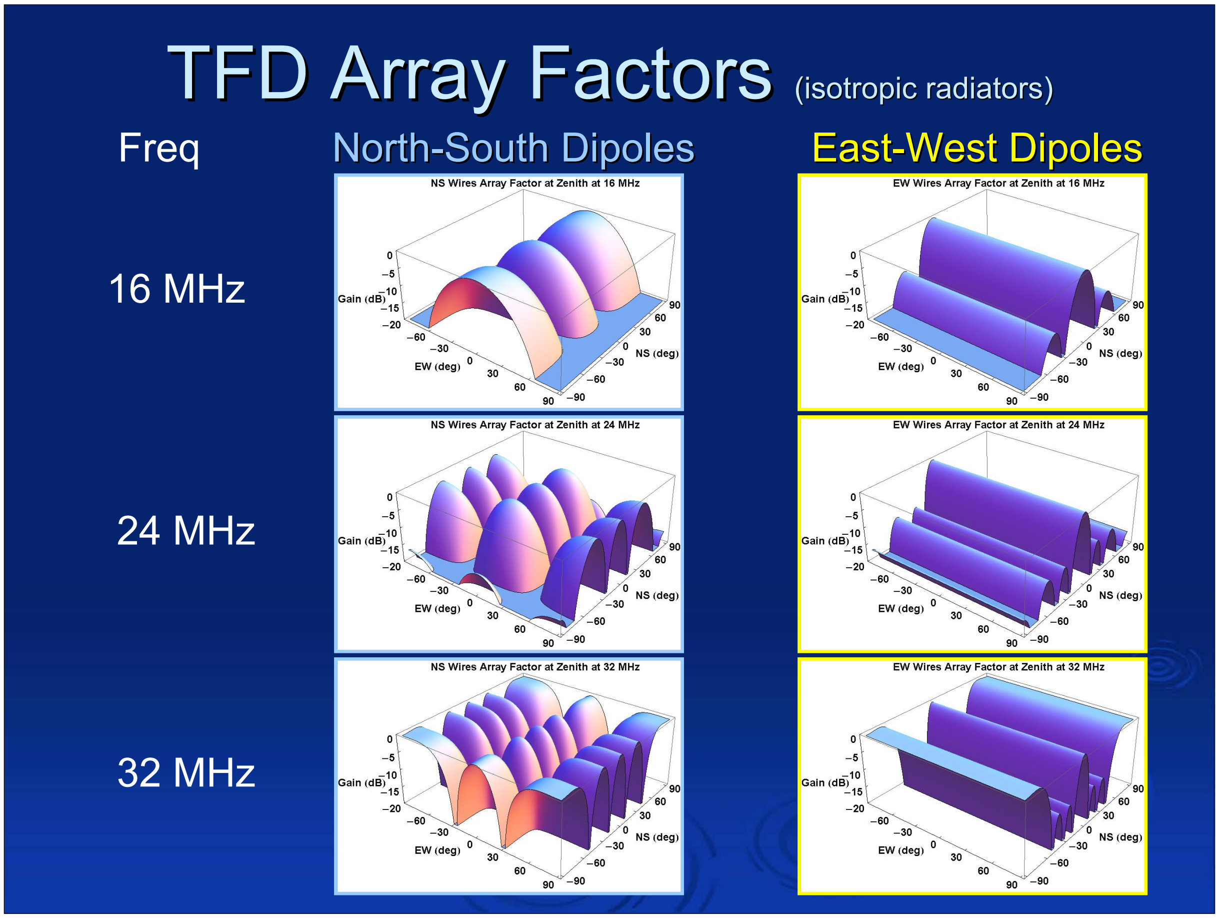

Here are the array factors for three frequencies. This represents the interference pattern formed by **isotropic radiators** in place of the real TFD elements of the array.

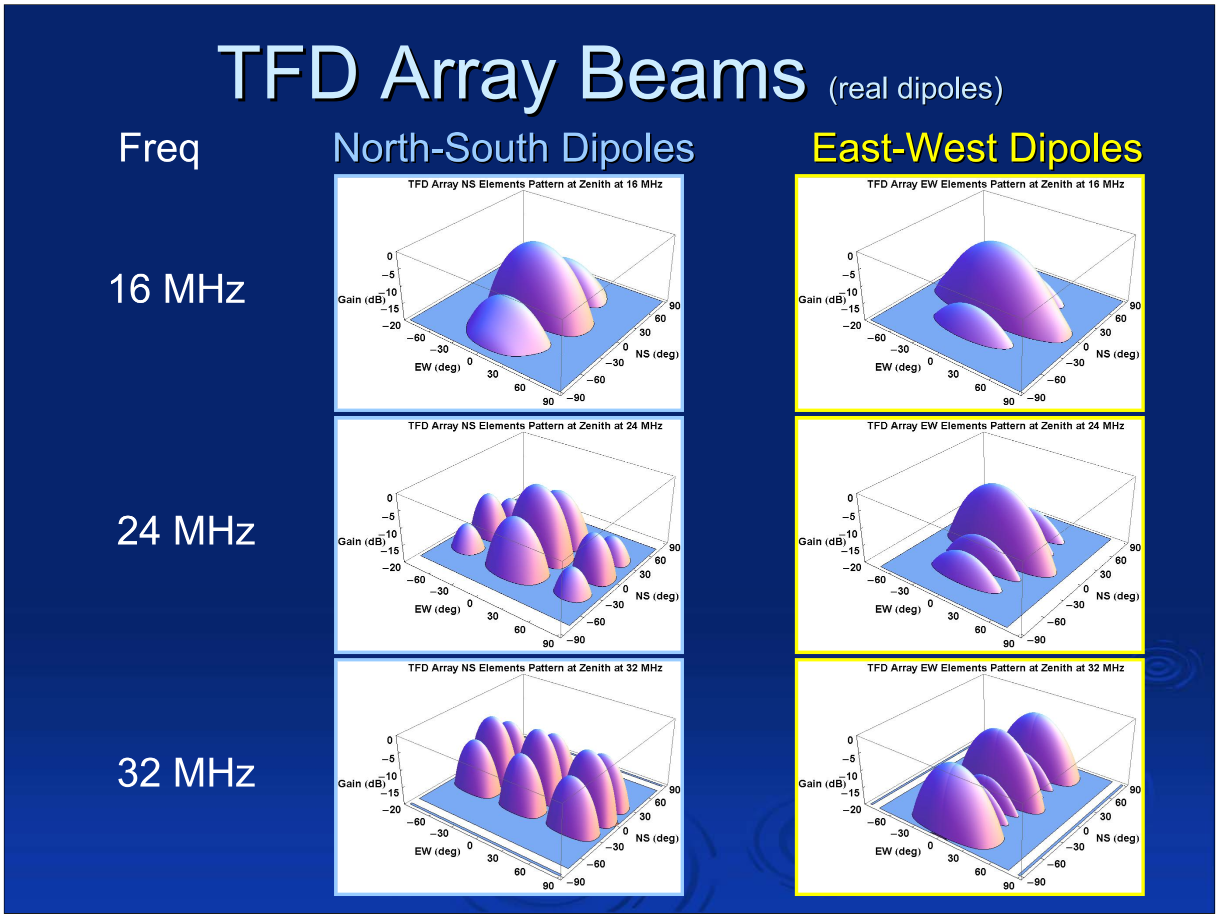

And here are the real beams (array steered to zenith), found by simply multiplying the array factors by the element Factors. This is **much** easier than running the electromagnetic field calculations for eight real TFD antennas spaced 32 feet apart in a rectangular array.

Note presence of grating lobes, especially at 32 MHz (bottom two plots). This happens because the elements are too far apart. Interferometers WANT these lobes, they are the desired product, and the elements in an interferometer are spaced much further apart than one wavelength. Phased arrays DO NOT WANT these lobes, and the element spacing should be less than half a wavelength. In the TFD array, the spacing is 32 feet — but one wavelength at 32 MHz is only about 31 feet. Thus, the desired element spacing (to prevent grating lobes) is anything less than about 15 feet — but the elements are 30 feet long, requiring at least 32 feet of space between them in a square array. Thus, grating lobes exist in the TFD array at all frequencies being used (16 to 32 MHz), but the ones at the higher frequencies are particularly strong. The grating lobes at lower freqs are somewhat attenuated due to the beam pattern of the individual elements.

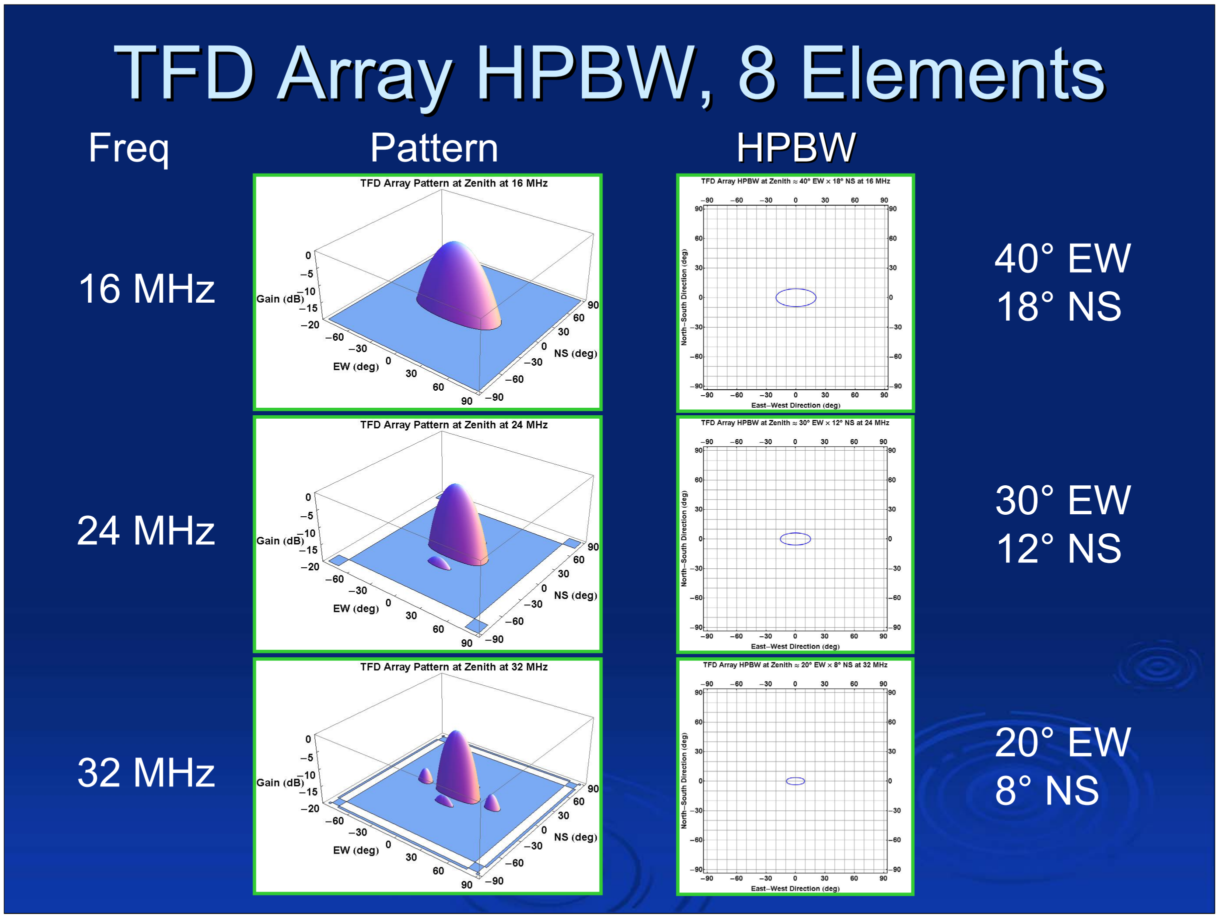

Plots are for a **beam at zenith** (no delay cables). That is, these beams represent the yellow and blue arrays multiplied together.

Here are the yellow and blue responses multiplied together to get the overall 8-element array response (at zenith!).

This is valid for the RCP output observing an RCP source (or LCP out observing an LCP source), or the summed EW & NS dipoles observing a randomly polarized source (without a hybrid to generate CP).

These plots and HPBW's, however, still don't tell the full story of the TFD array. We need to see what happens when we steer the beams of the yellow and blue arrays with delay cables.

Who know how to point the yellow and blue arrays. And we know what their response patterns are.

Since we must combine the signals from the yellow and blue arrays to generate circular polarization, **how does beam steering affect the circularly polarized signal that is generated?**

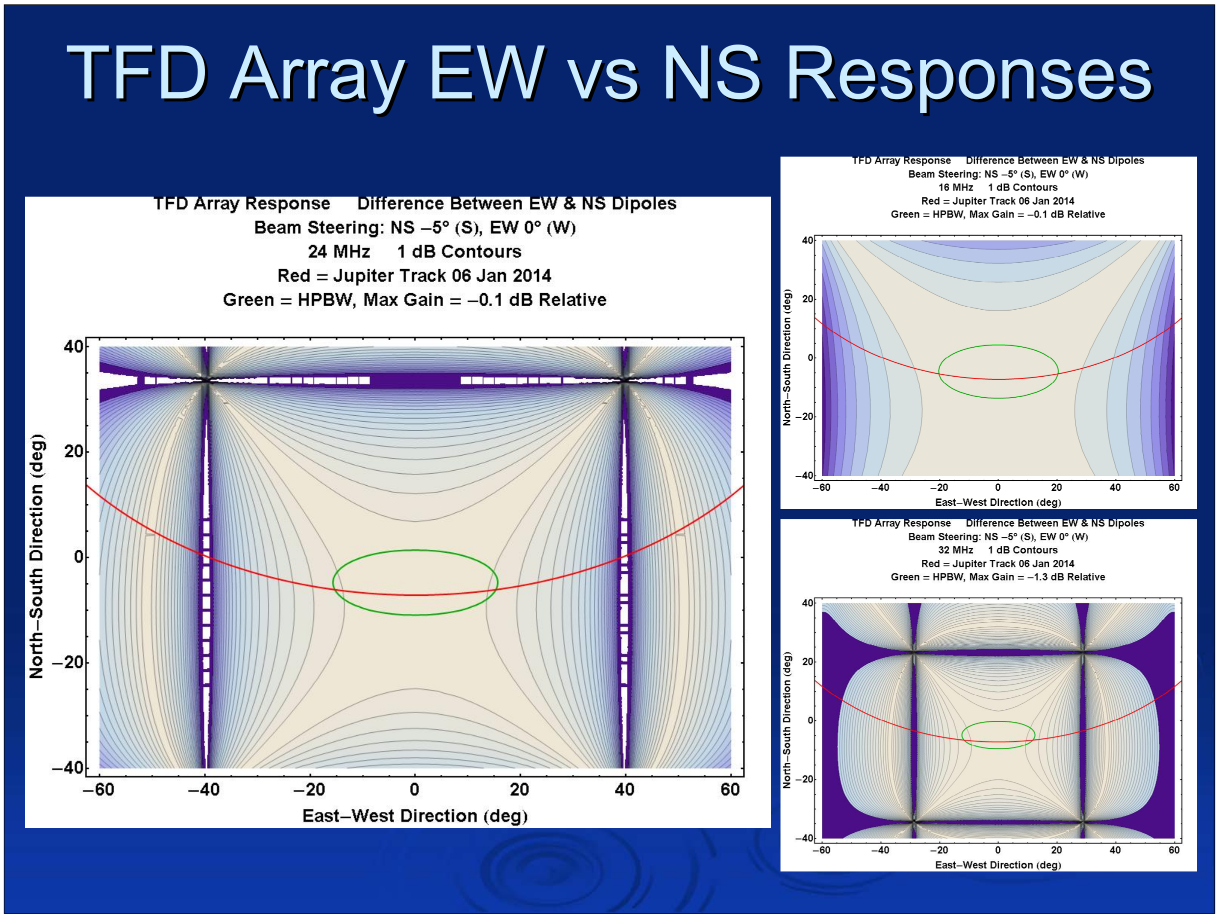

LEFT: 24 MHz. Upper Right: 16 MHz. Lower Right: 32 MHz.

These plots show the **difference** in the responses of the TFD array's NS wires (blue array) and its EW wires (yellow array) as the source moves off axis in the E/W or N/S directions. That is, these plots are for a **the array steered 5°S (AZ 180°, EL 85°).**

Since we derive RCP and LCP from these orthogonal linear elements, it is important to know how far off-axis the source can be while still maintaining a nearly equal response in both sets of elements.

As can be seen at each frequency, the portion of the beam where there is less than 1 dB difference in the responses of the NS and EW wires is **greater** than the HPBW of the **whole array** (slide 39). For zenith steering, as long as the source is within the HPBW, it is also in the area where the difference between the two linear responses is less than 1 dB.

TFD Array EW vs NS Responses

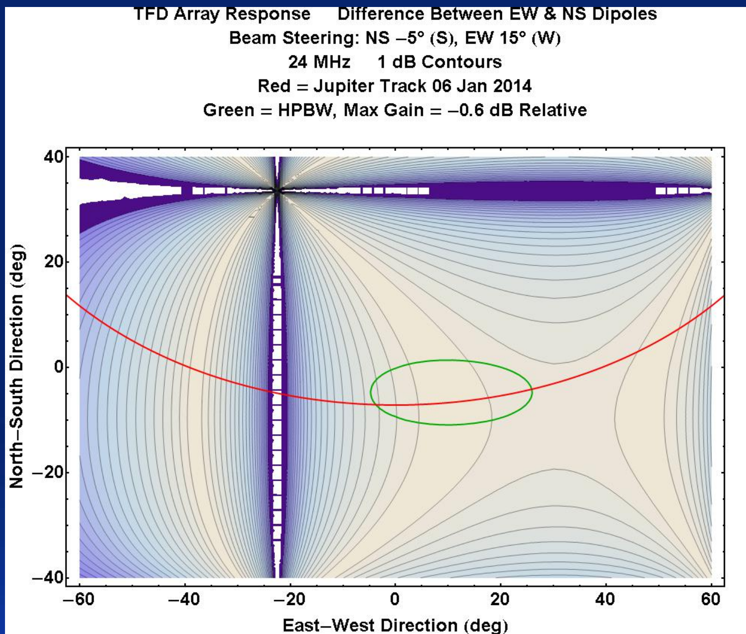

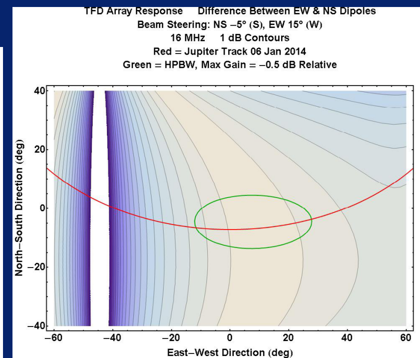

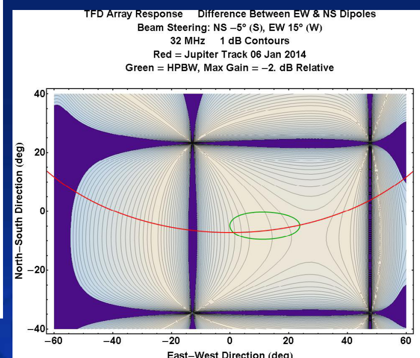

LEFT: 24 MHz. Upper Right: 16 MHz. Lower Right: 32 MHz.

Array steered 5°S, 15°W (AZ 252°, EL 74°)

The **difference** in the responses of the EW versus NS elements is getting **larger**!.

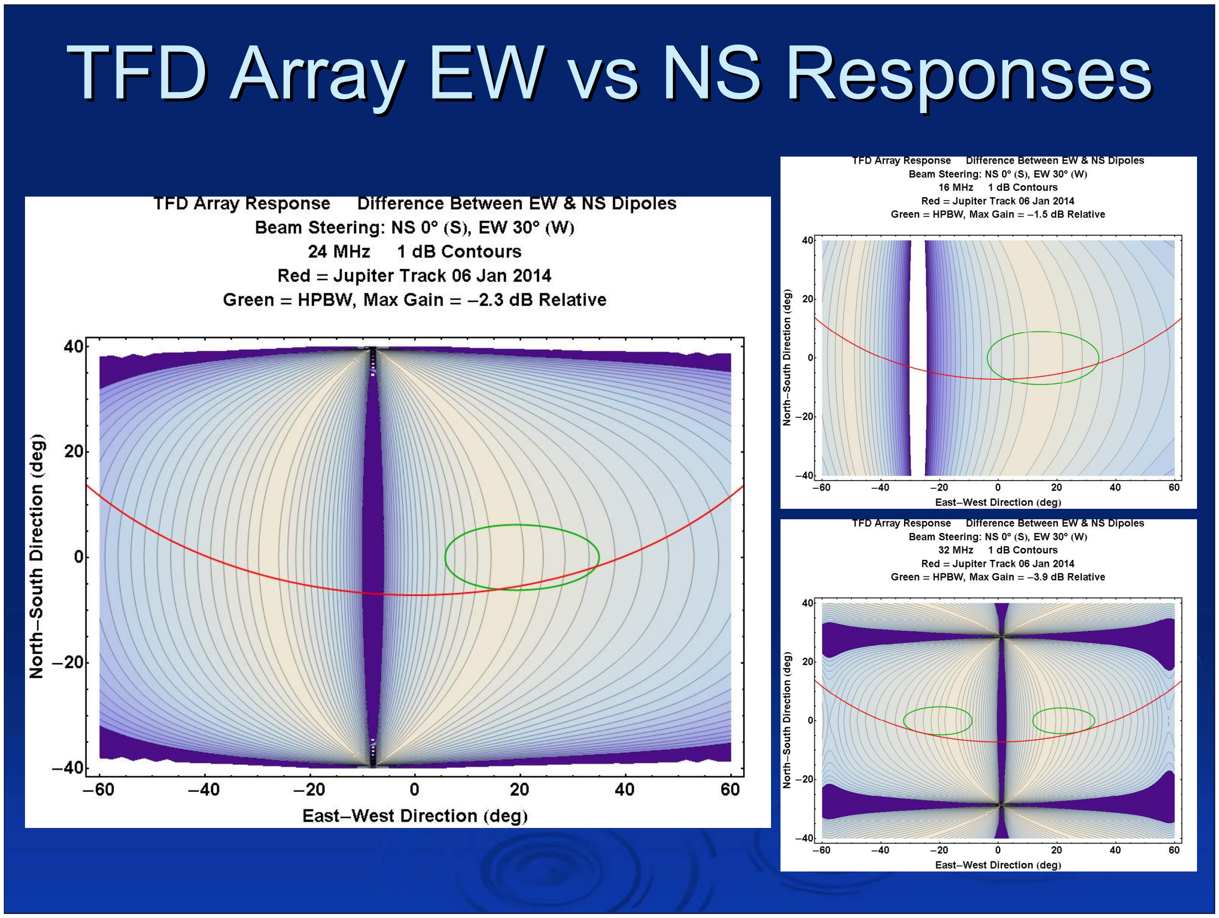

LEFT: 24 MHz. Upper Right: 16 MHz. Lower Right: 32 MHz.

Array steered 30°W (AZ 270°, EL 60°)

The **difference** in the responses of the EW versus NS elements continues to get **larger**.

Note that the EW beam steering does NOT completely determine the actual location of the overall beam. The NS wires are aimed 30° west, but the EW wires are still at zenith (one cannot beam steer a single row of wires in the plane normal to the row). The net effect is that the EW wires pull the overall beam back towards the meridian.

A difference in NS and EW element responses can be seen as Faraday banding in a spectrogram. As this slide indicates, the TFD array is much more sensitive to this at higher frequencies. Therefore, if the source is somewhat off-axis, we expect Faraday banding to be stronger (deeper nulls) at higher frequencies. We'll see an example of this shortly.

The Math

Response of array $= G(\theta,\phi) = G_{AF}(\theta,\phi)\ G_{EF}(\theta,\phi)$

where

$$G_{AF}(\theta,\phi) = \frac{\sin^2\left[N\pi\left(\frac{d_{NS}}{\lambda}\right)(\sin\theta - \sin\alpha)\right]}{N^2\sin^2\left[\pi\left(\frac{d_{NS}}{\lambda}\right)(\sin\theta - \sin\alpha)\right]}\ \frac{\sin^2\left[M\pi\left(\frac{d_{EW}}{\lambda}\right)(\sin\phi - \sin\beta)\right]}{M^2\sin^2\left[\pi\left(\frac{d_{EW}}{\lambda}\right)(\sin\phi - \sin\beta)\right]}$$

$G_{EF}(\theta,\phi) =$ Element factors (fitted curves)

where

$\theta =$ Source angular distance from zenith in the north-south direction

$\alpha =$ Beam steering angle from zenith in the north-south direction

$N =$ Number of elements in the north-south direction

$d_{NS} =$ Distance between array elements in the north-south direction

$\phi =$ Source angular distance from zenith in the east-west direction

$\beta =$ Beam steering angle from zenith in the east-west direction

$M =$ Number of elements in the east-west direction

$d_{EW} =$ Distance between array elements in the east-west direction

$\lambda =$ RF wavelength

For those who really want to know how to do these calculations, here are the equations used to calculate the response of a uniformly illuminated rectangular array of uniformly spaced elements.

Ref. Skolnik, “Introduction to Radar Systems”, McGraw-Hill (1962), section 7.7 < **https://archive.org/details/IntroductionToRadarSystems** >

G_AF = Array Factor

G_EF = Element Factor

The contours in the plots on slides 45–47 were made by calculating separate gain factors for the yellow and blue array sections (slides 32 & 33), then finding the absolute value of the difference between them.

The HPBW’s in the plots on slides 43–47 were determined by calculating a combined gain factor for the yellow & blue array sections, then finding the contour that was 3 dB down from peak. NOTE: slide 44, the SuperJove configuration, is simply the east-west wires (yellow section) of the TFD array by themselves.

See also: Longbrake, “True Time Delay Beam Steering for Radar”, USAF < **http://www.microwaves101.com/downloads/Longbrake%20-%20TTD%20for%20Radar.pdf** >

DPS System General Specs

- Useful beam steering up to ~30° from zenith
- Zenith directivity TBD (~14 dBic?)
- 16 to 33 MHz coverage
- 7.5, 15, 30, & 60 kHz wide IF BW's
- 40+ dB dynamic range
- ~5 dB noise figure (~625 K) (Theoretical)
- 2 ksamp/sec x 2 sides, correlated samples
- 12-bit resolution, $\Delta T \approx 500\ \mu s$ per sample
- 200 to 500 freq channels each side
- Sweep rate 4 Hz to 10 Hz each side

DPS Observations

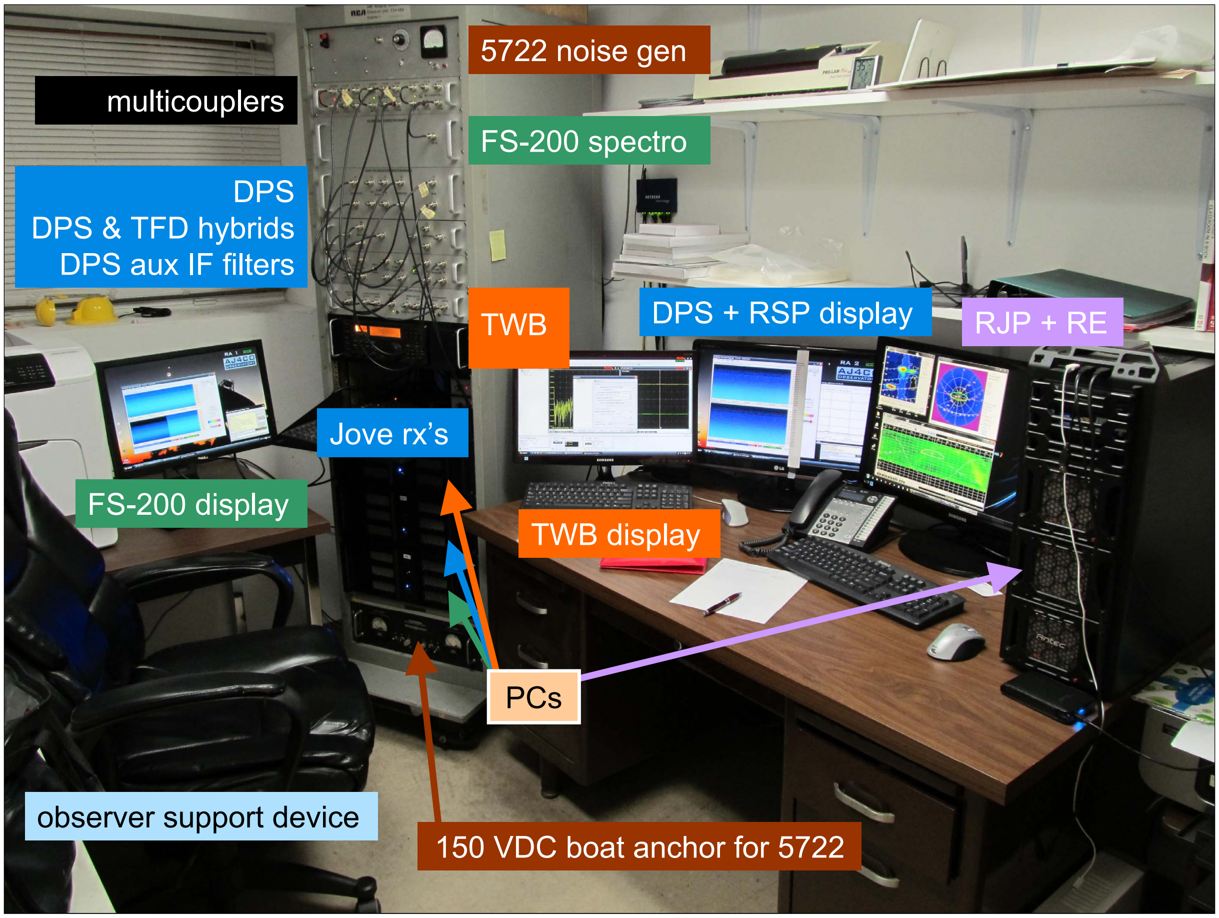

DPS installed in a 19" rack. AJ4CO Observatory, High Springs, Florida.
DPS system component labels in blue.

DPS Observations

29 Dec 2013, Io-A

15° off-axis (beam @ zenith)

No Faraday banding

RCP

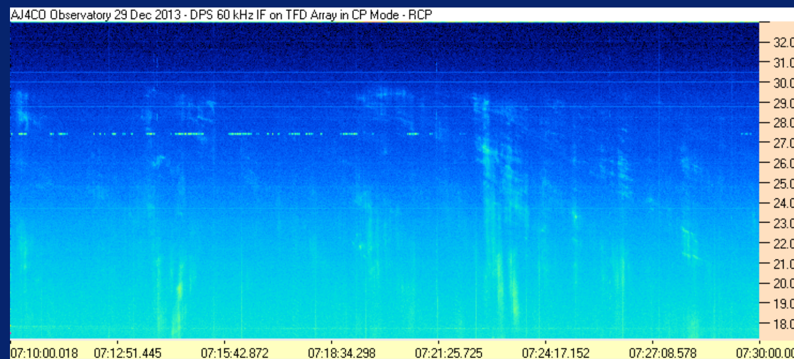

LCP

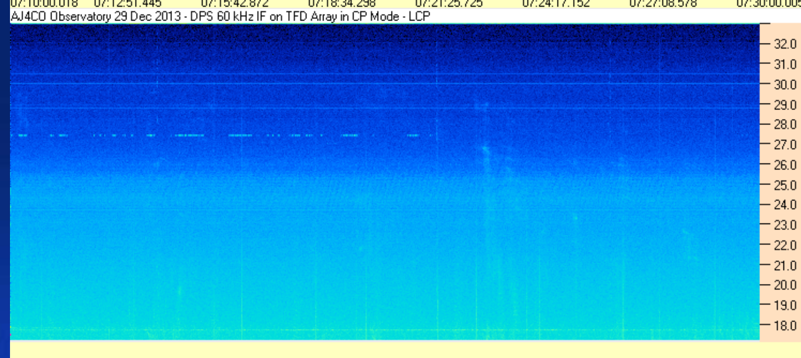

DPS Observations

29 Dec 2013, Io-C

50° off-axis (beam @ zenith)

Lots of Faraday banding

Illustrates difference between yellow and blue array responses

RCP

LCP

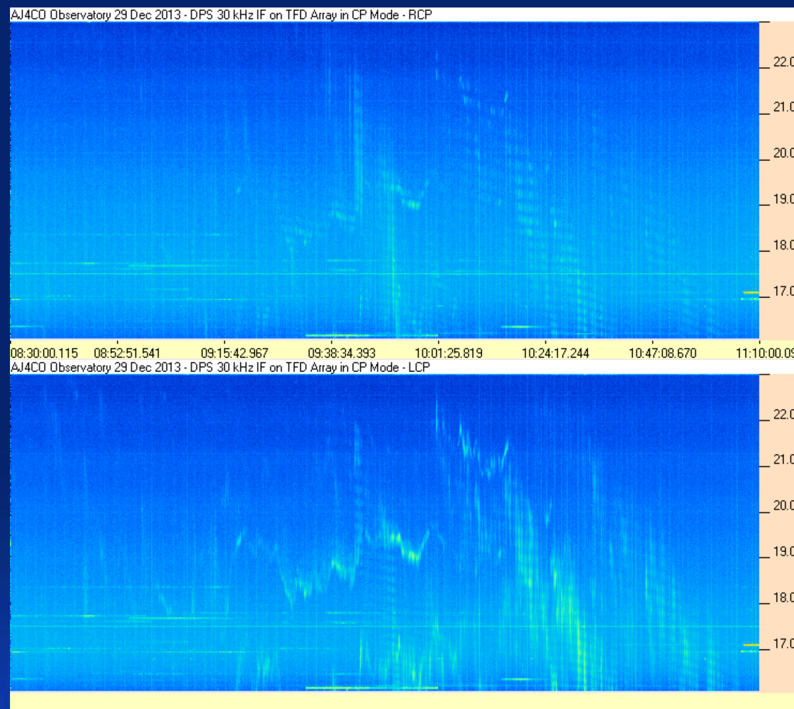

DPS Observations

23 Jan 2014, Io-A/C

10° off-axis (beam @ zenith)

Io-A RCP

and

Io-C LCP

RCP

LCP

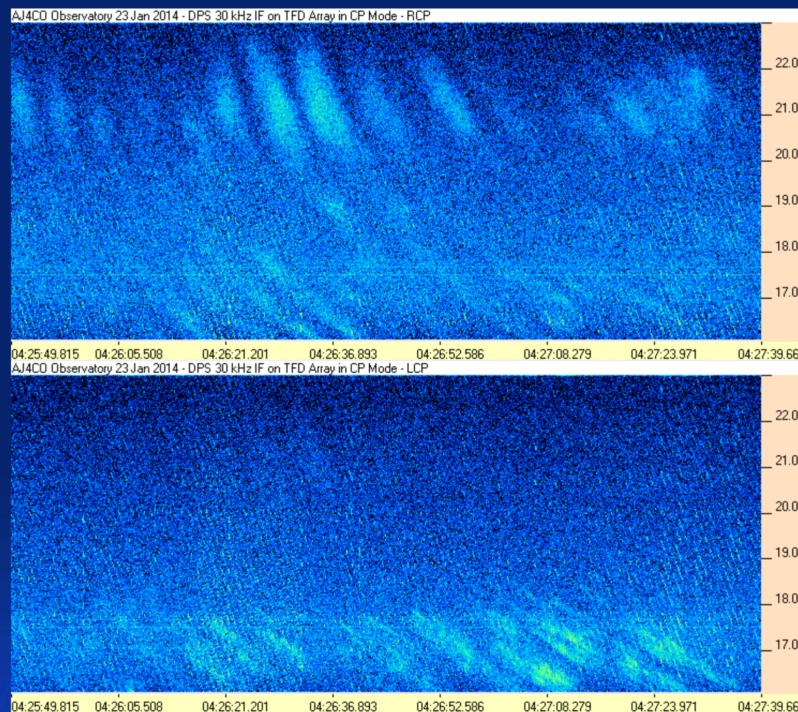

Shows that polarization can be used to de-confuse the decametric emission sources.

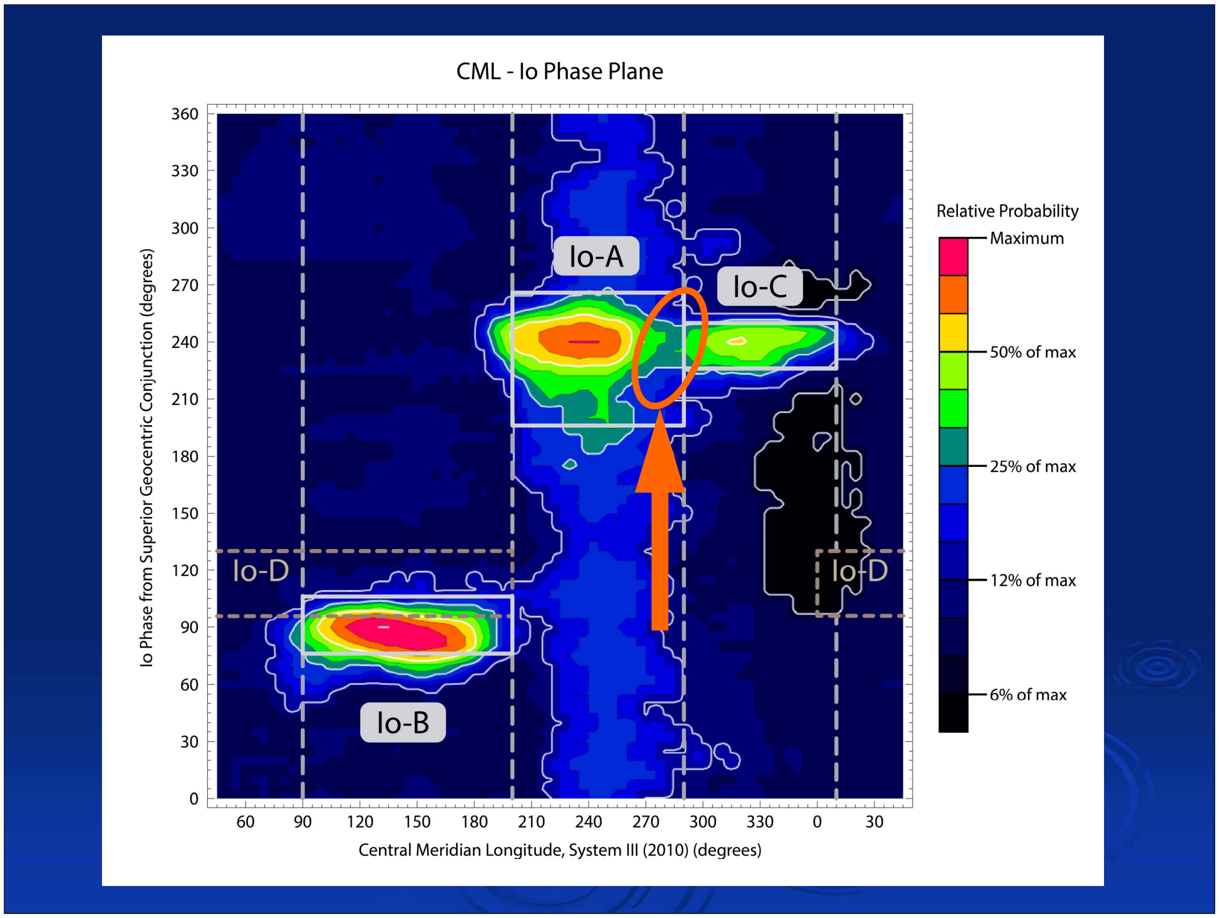

When Jupiter and Io are near this region of the phase plane, we often see emission from the Io-A (RCP) and Io-C (LCP) at the same time.

DPS Observations

23 Jan 2014, Io-A/C

10° off-axis (beam @ zenith)

Io-A RCP

and

Io-C LCP

RCP

LCP

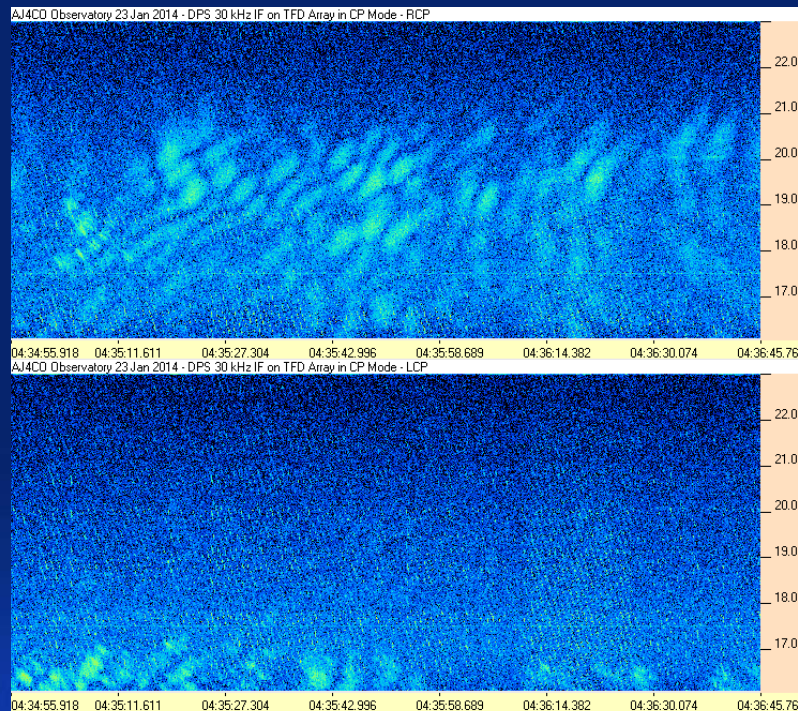

Shows that polarization can be used to de-confuse the decametric emission sources.

DPS Observations

23 Jan 2014, Io-A/C

10° off-axis (beam @ zenith)

Io-A RCP

and

Io-C LCP

RCP

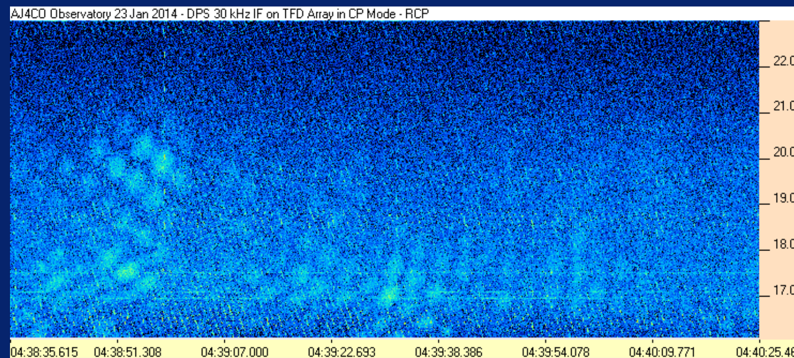

LCP

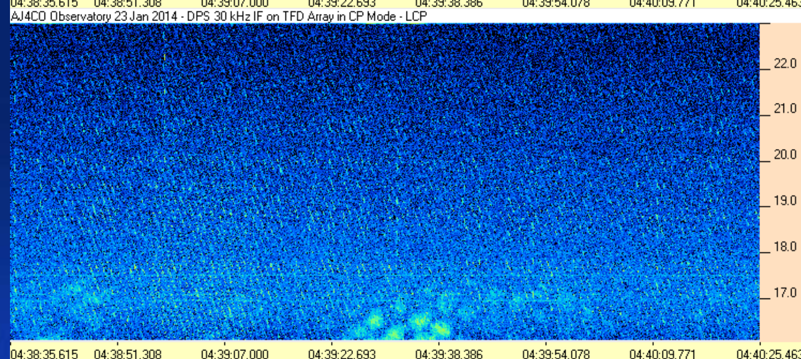

Shows that polarization can be used to de-confuse the decametric emission sources.

DPS Observations

24 Jan 2014, Io-B

10° off-axis (beam @ 5S 30W) @0615 UTC

Io-B RCP

and

Io-D(?) LCP

RCP

LCP

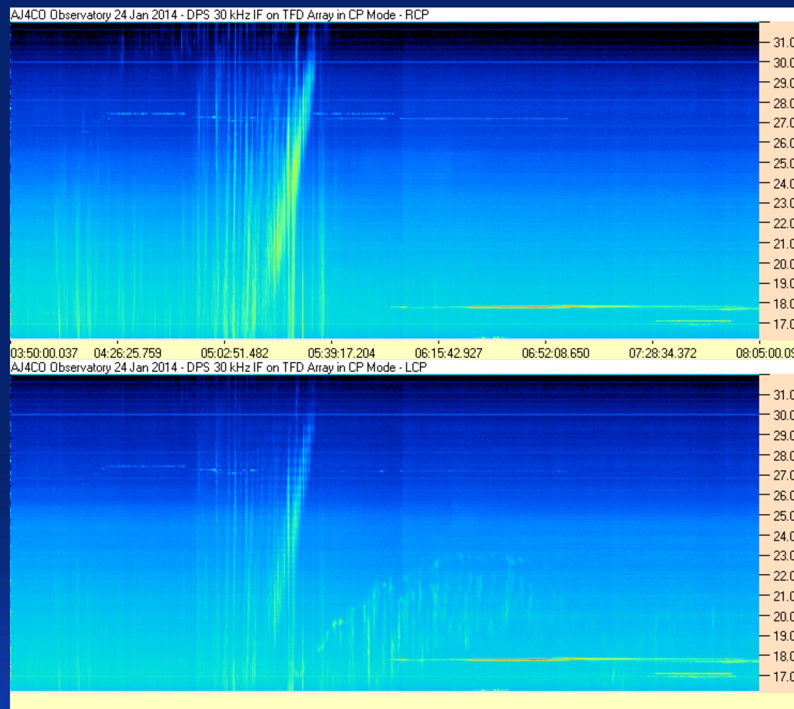

Shows that polarization can be used to de-confuse the decametric emission sources.

DPS Observations

24 Jan 2014, Io-B

10° off-axis (beam @ 5S 30W) @0615 UTC

Io-B RCP

and

Io-D(?) LCP

RCP

LCP

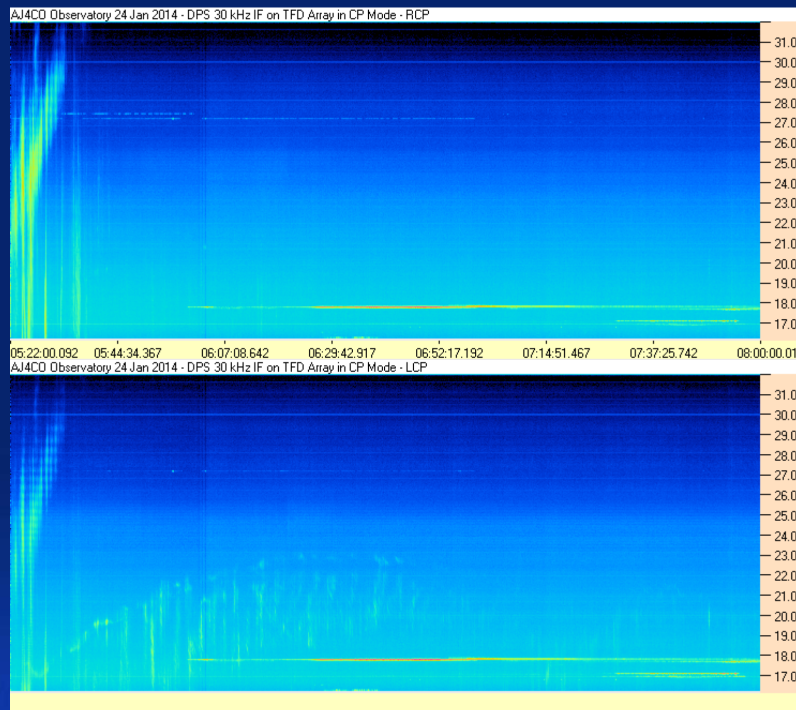

Shows that polarization can be used to de-confuse the decametric emission sources.

DPS Observations

24 Jan 2014, Io-B

5° off-axis (beam @ 5S 15W) @0504 UTC

Io-B RCP dominant

RCP

LCP

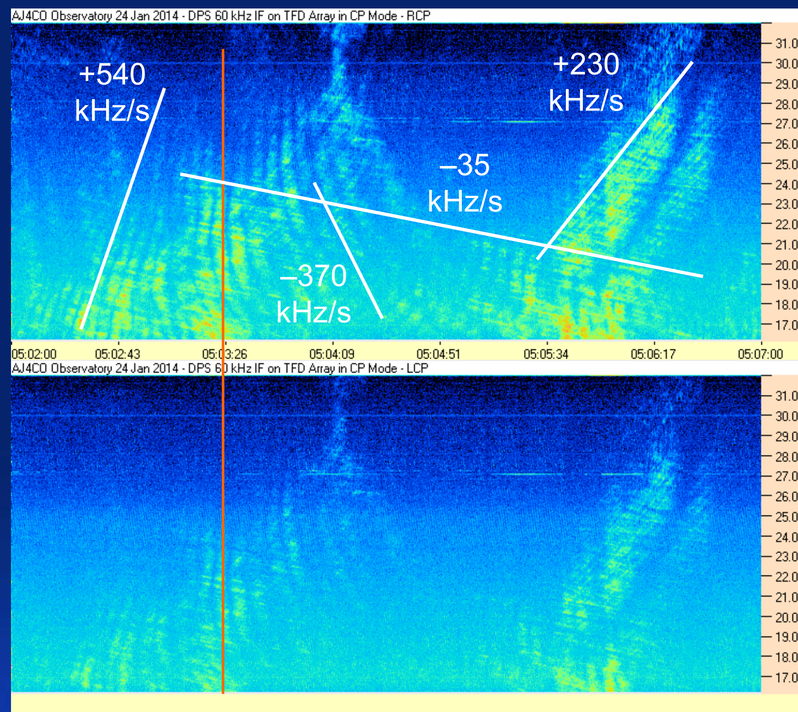

The lane peaks in this spectrogram occur at the same time for RCP and LCP.

The steeper lanes are at first positive slope, then negative. Scintillation or modulation?

DPS Observations

04 Mar 2014, Io-B

6° off-axis (beam @ 5S 15W) @0300 UTC

Io-B RCP dominant

RCP

LCP

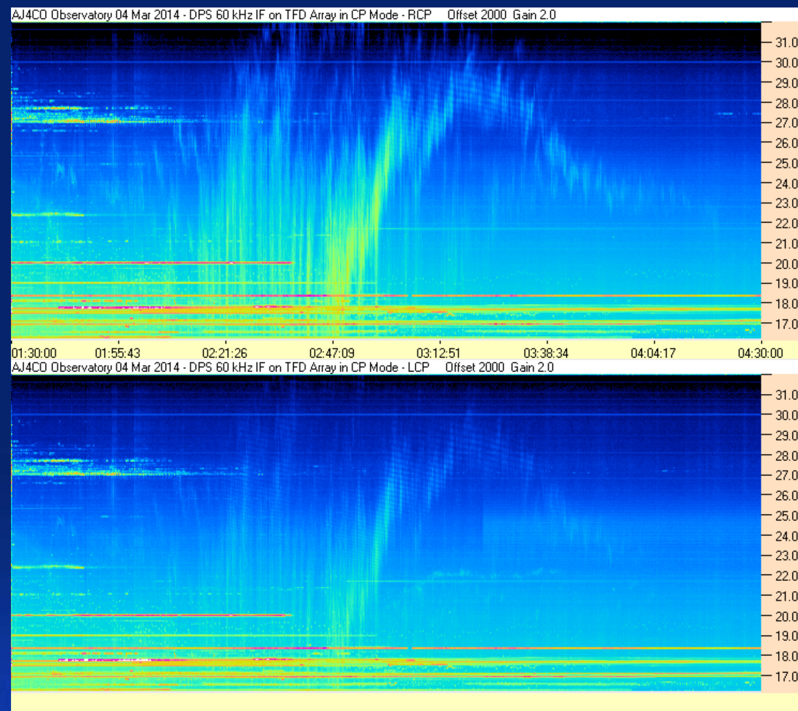

A very nice complete top half of an Io-B arc.

The faint broadband interference from 0320 UTC onward at around 24-25 MHz appeared when an SDR-14 was connected to one of the multicouplers.

DPS Observations

04 Mar 2014, Io-B

4° off-axis (beam @ 5S 15W) @0250 UTC

Io-B RCP dominant

RCP

LCP

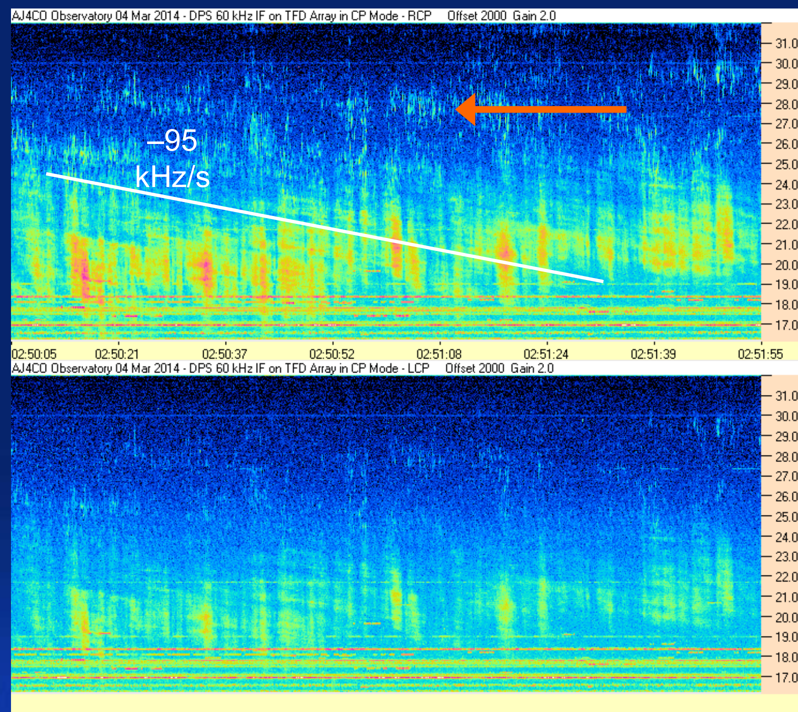

Arrow indicates S bursting. The DPS was use to determine where to tune the TWB to obtain high speed spectrograms of S bursts.

DPS Observations

04 Mar 2014, Io-B

10° off-axis (beam @ 5S 15W) @0320 UTC

Io-B RCP dominant

w/ LCP Io-D N event?

RCP

LCP

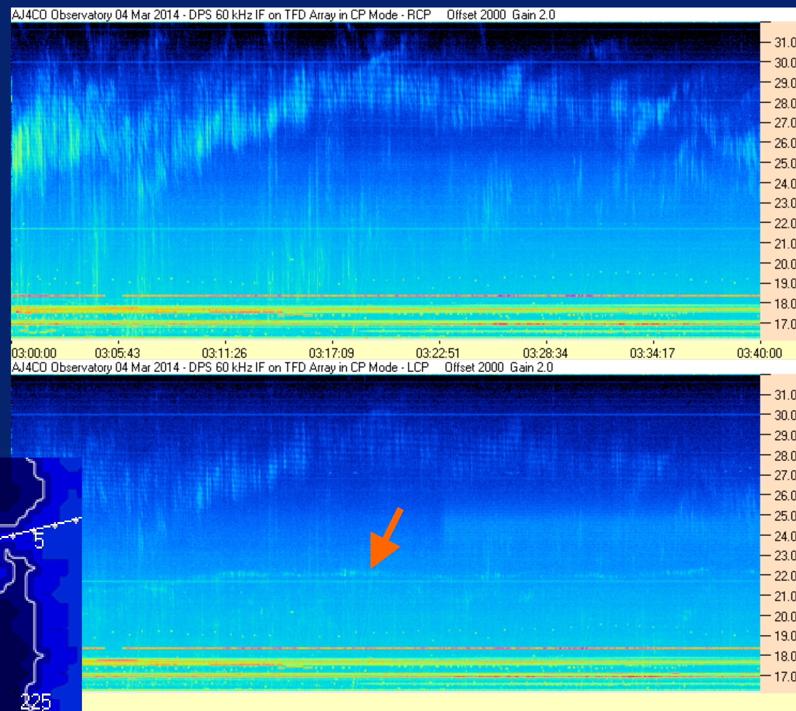

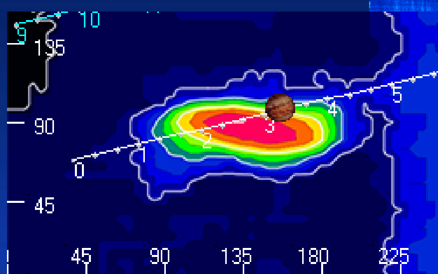

What’s this LCP N event doing here? Who ordered that? Is this Io-D?